EXPLORATION OF MICROPLASTIC FIBERS TRANSPORT DYNAMICS IN POROUS MEDIA USING A COMBINATION OF PHYSICAL EXPERIMENTS AND NUMERICAL SIMULATIONS

By

TYLER T. FOUTY

A dissertation submitted in partial fulfillment of
the requirements for the degree of

DOCTOR OF PHILOSOPHY

WASHINGTON STATE UNIVERSITY
Department of Civil and Environmental Engineering

MAY 2024

To the Faculty of Washington State University:

The members of the Committee appointed to examine the dissertation of TYLER T. FOUTY find it satisfactory and recommend that it be accepted.

Nick Engdahl, Ph.D., Chair

Lazaro Perez, Ph.D.

Courtney Gardner, Ph.D.

Jan Boll, Ph.D.

Alex Fremier, Ph.D.

ACKNOWLEDGMENTS

My dissertation has been a great learning process. The support I have received from my mentors, family, and friends made it all possible. First, I want to acknowledge the funders that supported me: the National Science Foundation Graduate Research Fellow Program, Washington State Department of Transportation, and Washington State University- Research Assistantships for Diverse Scholars. I want to thank my advisor, Dr. Nick Engdahl, for all your guidance, words of encouragement, and support during this process. I also want to thank Dakota Donaldson and Joshua Pridemore for there help with the literature review and developing the experimental methods. I want to thank my committee members for their guidance over the years and my family for their love and support.

EXPLORATION OF MICROPLASTIC FIBERS TRANSPORT DYNAMICS IN POROUS MEDIA USING A COMBINATION OF PHYSICAL EXPERIMENTS AND NUMERICAL SIMULATIONS

Abstract

by Tyler T. Fouty, Ph.D.
Washington State University
May 2024

Chair: Nick Engdahl

The existence of microplastics (MPs) in the environment has been a growing concern for two and a half decades, having now been found in remote areas, ocean sediment, deserts, and mountain peaks. MPs in the environment are a concern because they can impact soil properties and organisms. Research has determined that MPs can affect aquatic organisms in two forms: 1.) mechanical- MPs can attach to the body of the organism and impact their movement and 2.) chemical- the leaching of chemicals from the MPs can be absorbed by the organisms, both of these impact forms can lead organisms to experience inflammation, stress, death, and reproduction decline. The impact on human health is limited but assumed to see the same impacts as aquatic organisms. The largest MP type by mass found in the environment is microplastic fiber (MPF). Scientists understand where MPs come from and where they

end up (large-scale movement), the missing aspect is how they move. This research gap is missing due to the transport mechanics occur at the pore scale which is difficult to capture. The mechanisms of MPFs transport have been proposed numerically but have not been validated. This research collected MPF transport data in a 2D laboratory model to understand the transport dynamics in porous media of three different lengths 0.3, 0.5, 0.8 cm and microbeads to act as a passive tracer, modeling MPF transport with existing simulation tools (ADE equation) and validate the only MPF distributed simulation model to date. Videos captured the trajectory of the fiber and beads, and the trajectory data was used to generate breakthrough curves. The experimental data found that fibers tumble/roll during their transport through the model, that fibers traveled much slower than expected, and longer fibers would travel slower. It was observed that fibers would have an abrupt change in velocity and became stuck then re-mobilized. This paper refers to this dynamic as "trapping". Comparisons to the ADE (i.e. advection-dispersion models) equation and the distributed simulation model (DSM) were unable to simulate MPF transport, which leads to the question of what dynamics are missing from the models. ADE simulation was unable to capture the correct shape of the curve, with particles arriving sooner than the experiments. The DSM can simulate the transport of beads but nothing else. This suggests that the missing dynamics result in a retention or trapping process, but the design of these experiments cannot determine the precise mechanism. However, two upscaled repre-

sentations of the trapping process were able to significantly improve the agreement of the experimental and numerical results.

TABLE OF CONTENTS

Page

ACKNOWLEDGMENTS iii

ABSTRACT iv

LIST OF TABLES viii

LIST OF FIGURES ix

CHAPTER 1

1. TRANSPORT BEHAVIORS OF MICROPLASTIC FIBERS IN POROUS MEDIA USING MESO-SCALE EXPERIMENTS 1

1.1 Introduction 1
1.2 Background 7
1.3 Methodology 21
1.4 Results 28
1.5 Discussion 37
1.6 Development of this project 46
1.7 Conclusions 49

BIBLIOGRAPHY 51

LIST OF TABLES

Table Page

1.1 Best fit values of ADE simulation for all particles for pore 1 40

1.2 Gamma values for DSM waiting time simulation for all particles for pore 1 43

LIST OF FIGURES

Figure Page

1.1 Life cycle of a typical MP 3

1.2 Plan view of the meso-model. All the dimensions in the figure are in centimeters. The flow will enter the model from the left and exit on the right. The middle two pores are the focus of the study. 23

1.3 The experimental rig that houses the meso-model. The water inlet is on the left, and the outlet is on the right side of the rig. The injection point is where the syringe is connected to the supply line to introduce the fibers and beads into the flow field. All measurements are in centimeters. 26

1.4 2D simulation of the velocity field in the meso-model. The velocity of the water increases in the narrow sections and decreases in the large void spaces between pores. 28

1.5 This figure is a composite of three different fibers multiple times through the meso-model. This composite provides a visual demonstration of the experimental results. One fiber travels above both pores, another travels below both pores, and the last fiber travels below the first and above the second pore. Each fiber tumbles/rolls in large pore openings. 30

1.6 This figure shows the trajectories of 300 particles for each fiber length and beads. These trajectories show that fibers and beads will switch travel zones between pores; the occurrence decreases with the increase in fiber length. The beads' trajectories are in a thinner band than the fibers, subjecting them to the velocity field's faster section. 31

1.7 These graphs show the BTC for pore one and both pores. The BTCs are normalized by the mean breakthrough time for the beads. Fibers move slower than beads. 8mm length fibers are the slowest moving fibers; 3 mm and 5mm fibers have similar travel times. 32

1.8 These figures show the BTCs for the four models used to simulate MPF transport. The ADE simulation (a) can capture the middle of the beads and the last 0.7 of the fiber curves but has beads and fibers moving faster than the experiments at the front of the curves and the tail for the beads. The distributed simulation model (b) does a very good job of simulating the transport of beads, but the simulation had fibers with a similar arrival time as the experimental beads. The simulation can capture the dynamic of $3mm$ and $5mm$ fibers having similar travel times and $8mm$ fibers traveling slower. The distributed simulation model with waiting time (c) produces BTCs similar to the experiments. The distributed simulation model with trapping (d) has similar BTCs as the experiments tell 0.8; trapping starts to over-predict and has a slower arrival time for all fibers. 35

1.9 This figure shows the waiting time distribution for each fiber length. The $8mm$ fibers jump in the middle of the curve while the 3 and $5mm$ stay the same. 42

Dedication

This dissertation is dedicated to my family who

provided love and support during this journey

CHAPTER 1. TRANSPORT BEHAVIORS OF MICROPLASTIC FIBERS IN POROUS MEDIA USING MESO-SCALE EXPERIMENTS

1.1 Introduction

The environment is seeing a massive influx of plastic yearly. Plastic can be observed on the side of roads, floating in rivers, lakes, and the ocean, which is currently the home of a 1.6 million square kilometer garbage patch [Lebreton et al., 2018]. Plastic production in 2019 was 370 million tons [Halfar et al., 2021] and only 9 percent of plastic since the 1950s has been recycled [d'Ambrières, 2019]. Since its fabrication, synthetic plastic has become integral to the human experience and ubiquitous in society; from materials on our clothes and shoes to parts of cars and bikes, cell phone cases, umbrellas, coffee cups, bags, children's toys, etc., we are surrounded by plastic. These are all examples of macroplastics, which are easy to see with the naked eye, but Microplastics (MPs) are an even more significant, growing concern in the modern pollution conversation. Much of their danger is thought to lie in their size (typically less than 5 millimeters) and mobility since they can pass through many wastewater treatment plants (WWTP) [Alvim et al., 2020, Murphy et al., 2016]. As a result, a

large volume of the 370 million tons of plastic has been found in different environment [Auta et al., 2017, Andrady, 2011], rivers [Blettler et al., 2018, Ghayebzadeh et al., 2021, He et al., 2021], soil [Kim et al., 2021, Qi et al., 2020, Chae and An, 2018], the atmosphere [Akdogan and Guven, 2019, De Falco et al., 2020, Peller et al., 2019], and even in the human bloodstream [Park et al., 2020]. MPs are being produced at a high rate, both from manufacturing and the breakdown of existing plastics, so their quantity in the environment is increasing at an alarming speed. Over the past decade, MPs have been a growing subject of interest, with oceans being the primary focus. The study of MP has moved inland (rivers, lakes/reservoirs, and terrestrial soil) since they are the logically expected sinks for MPs inland in the last few years [Eerkes-Medrano et al., 2015, Carr et al., 2016, Blettler et al., 2018, Boyle and Örmeci, 2020]. Research has looked at their movement/transport (big picture Figure 1), effects on environmental organisms, and locations of sinks (soil, rivers, lakes, ocean sediment), and the general conclusion is that sediment is MPs' final sink [Halfar et al., 2021].

Microplastics have been found in high quantities in the environment, but their long-term impacts remain unknown [Waldschläger et al., 2020]. There is speculation about MP's being carcinogenic and the danger of MP's picking up toxic metals [Park et al., 2020] but as before, strong suspicions are not direct evidence. Much analysis has been committed to quantifying MPs in environmental samples [Alimi et al., 2018], but little knowledge of their nature exists. Some studies indicate they harm smaller

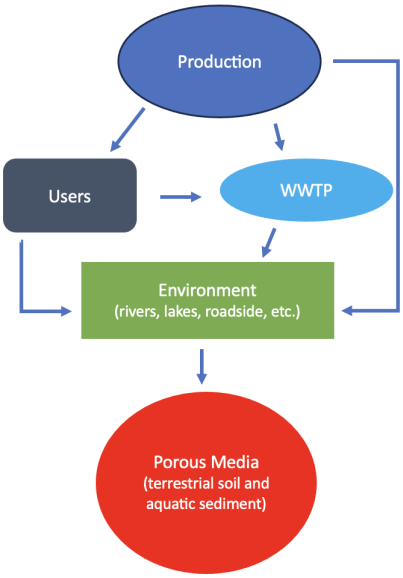

Figure 1.1: Life cycle of a typical MP

organisms [Claessens et al., 2013] by reducing reproduction and lowering lifespan. Investigations are needed regarding bioaccumulation and whether MPs are transport vectors for viruses, toxic compounds, and by-products of MPs themselves before any concerns can be assessed [Birch et al., 2020, Harrison et al., 2018]. However, the assumption that MPs could be harmful implicitly implies that they are mobile in the environment or else they could not be transport vectors for anything. The question of mobility presently remains open because our current knowledge of MPs is essentially limited to studies reporting their existence at specific sites, experiments have looked at the infiltration of MPs in column of natural and simulated sediment and has not yet addressed how they move in detail [Gaylarde et al., 2021, Xiong et al., 2022, Athey et al., 2020, Dodson et al., 2020].

The MP transport dynamics has focused on particles of spherical shape, while microplastic fibers (MPFs), the most prominent MPs by mass has very limited data on transport dynamics. The limited data leads to their being a scarce numerical description of the transport dynamics. Recognizing this barrier, Engdahl [2018] created a numerical model that explicitly modeled microplastic fibers (MPFs), the most prominent MPs by mass, based on first-principle physics. The numerical simulations of fiber positions and orientations over time showed that MPFs moving through porous media likely exhibit size exclusion and, as such, can move faster than solutes. This work is thought to be the most realistic MPF simulations to date and offered the first hypotheses about the dynamics of their transport mechanisms, but the problem with these results is that they are entirely numerical; to the best of our knowledge, no direct observations of the dynamic behaviors of MPF fiber exist to date. Prior to this study, there was no direct observation of the mobility of MPF in porous media. Progress has only recently begun to be made in these areas, and studies are beginning to attempt to capture their movement. A column study using glass spheres to represent soil by Waldschläger and Schüttrumpf [2020] investigated the filtration rate of MPs; a range of sphere diameters were used to simulate different sediment types and O'Connor et al. [2019] used glass spheres represent soil to look at the infiltration depth of MPs after rain events. A column study by Cohen and Radian [2022] investigated the infiltration depth of two types of fibers (polyester and nylon) in quartz

sand. It was found that short fiber and fiber made of nylon infiltrated further in the column than long fibers and fibers made of polyester [Cohen and Radian, 2022]. These column studies provide information on the bulk infiltration rates of MPFs but do not provide trajectory data, meaning the specific question of how they are moving at a fundamental level cannot be resolved. A new study is needed to provide trajectories to validate the Engdahl [2018] model and build a working knowledge of important processes impacting MPF migration.

The objective of this research is to fill some fundamental knowledge gaps in an effort to develop a basic understanding of MPF transport dynamics in porous media using laboratory experimentation and numerical simulation. The core problem we address is that MPF transport models are all but nonexistent, and the only one that currently exists [i.e. Engdahl, 2018] has no experimental validation. Our approach was to create laboratory experiments that directly capture MPF motion using a pseudo-2D, idealized, periodic pore. The hypotheses that will be evaluated to support the objective are: H1- MPF transport mechanics are fundamentally different from those of dissolved solutes. The structure of MPF allows them to have the ability to tumble/roll/deform while in motion, and a less vigorous version of these dynamics are expected for MPF dynamics in porous media. The travel times will be dependent on the size of the particle and the longer the particle the slower it will travel. H2- Effective transport models can be defined for MPF using many common solute transport

models, but these may not be precise process-based analogs. This will be evaluated by comparing breakthrough curves of MPF and colloid passive transport data, each fit to various effective transport models, and validate the only MPF-specific simulation to date [i.e. Engdahl, 2018]. The experiment design is a scaled-up version of micromodels used in flow and transport studies [Karadimitriou and Hassanizadeh, 2012], where video capture and trajectory analysis have been used to understand the dynamics of bacteria, biofilms, solutes, and more [Lanning and Ford, 2002, Perez et al., 2022, Corapcioglu and Fedirchuk, 1999]. The experiments provide first of their kind, direct observations of MPF movement. The results also allow descriptions of effective (upscaled) transport behaviors to be made using a range of existing solute transport models (e.g., advection-dispersion equation). The results show that MPFs demonstrate different transport dynamics than passive tracers and that, after accounting for previously overlooked transport mechanisms, the Engdahl [2018] simulation approach provides a good representative model for the fibers used in these experiments. These results help enhance the knowledge of MPF transport and the tools used to evaluate the possible impact of MPFs on the environmental system.

1.2 Background

1.2.1 What are microplastics?

MPs are considered colloids that are in the size range of $0.1 - 5mm$ [Du et al., 2021, Kooi and Koelmans, 2019], and there are two sources of plastics: 1.) Primary- plastic made in this size range and 2.) secondary- plastic broken down from larger materials that can be in the shape of fragments, spheres, film, and fibers [Ding et al., 2021, Dodson et al., 2020, Halfar et al., 2021, Harrison et al., 2018, Auta et al., 2017, Kumar et al., 2021]. Microplastic fibers (MPF) come from textiles, personal care products, and other fibrous materials [Alvim et al., 2020, Schirinzi et al., 2017]. MPFs are characterized by their long, thin structure and uniform, narrow width [Liu et al., 2019a]. Fibers from all of these products are released throughout their lifespan, during the construction of the product, during use (wearing/ rubbing against objects, putting on/off, etc.), washing/drying, aging of the product, and exposure to the elements (sunlight, temperature, wind, etc.) [Auta et al., 2017, Boyle and Örmeci, 2020, Alipour et al., 2021]. One of the dangers of MPs is that they do not dissolve in water, so they do not behave the same way other microscopic solutes behave [Du et al., 2021]. MPs also have fewer chemically detectable properties than dissolved solutes, making them more challenging to quantify [Stanton et al., 2019].

MPs are also being fabricated in large quantities in industries where plastic is pro-

duced. Many MPFs result from the clothing industry [De Falco et al., 2020]. Companies that utilize plastic-based materials in their clothing production, like polyester and nylon, can release dangerous amounts of plastic microfibers into the environment. The release occurs mainly through washing machines, when such clothes are washed, where the friction imposed by washing strips off massive numbers of MPFs [Hartline et al., 2016]. Most MPFs are collected in the sludge in WWTPs, but 2-10 percent exit the effluent in secondary treatment facilities and this rises to above 20 percent for primary treatment-only facilities. WWTP sludge is used as fertilizer in some places, which releases the captured MPF into the environment [He et al., 2018]. The natural degradation of plastics in bodies of water through physical or chemical means can take hundreds, if not thousands, of years, so the degradation of MP's can progress even more slowly [Du et al., 2021], but this degradation can occur on the timescale of months when exposed to UV.

1.2.2 Where can microplastic be found?

Samples of MPs have been found across the globe. MPs are small enough to be carried by the wind, ocean currents, and water. MPs enter the terrestrial environment from sources including WWTP sludge, plastic mulching, littering, compost, street runoff, flooding, and the atmosphere [Halfar et al., 2021, Li et al., 2020, Petersen

and Hubbart, 2021, Yang et al., 2020]. Soil is considered a temporary sink for MPs unless/until disturbed and put back into motion (surface runoff, soil tilling, wind, etc.) [Boyle and Örmeci, 2020]. The origin of aquatic MPs are primarily synthetic textiles, tire wear, WWTPs, surface runoff, litter, and atmosphere [Auta et al., 2017, Birch et al., 2020]. WWTP standard practices already capture about 90 percent of the MPs, but the remaining 10 percent is still a significant MP source [Alvim et al., 2020].

MPF are the largest source of plastic found in the environment. Current global estimates are that 90 percent of the surface water has microplastics and that 91 percent of that plastic, by mass, comprises fibers [Gaylarde et al., 2021]. MPFs comprise 90 percent of plastic particles found in the Great Lakes sediment, and in suburban lakes are upwards of 87 percent [Athey et al., 2020]. The amount of MPs in a stream was found to increase downstream of large population centers [Dodson et al., 2020] due to the increased plastic discharge from urbanization. Xiong et al. [2022] conducted a microplastic study on Flathead Lake in Northwest Montana, the largest freshwater lake by surface area in the Western United States. Surface water samples were collected at twelve locations across the lake. The recovered MPs were mostly microplastic fibers ranging from 55-99 percent of the MPs, with an average of 80 percent [Xiong et al., 2022]. Other studies confirmed that microplastic fibers end up in the sediment: notable examples of high MPF mass fractions are 90 percent

of particles in the Great Lake sediment [Athey et al., 2020], 86 percent of particles found in the arctic sediments [Athey et al., 2020], and 80 percent of MPs in beach sediment worldwide were fibers [Dodson et al., 2020].

1.2.3 Microplastic Transport

Due to their size and shape, MPF's have penetrated a wide range of environments, from the terrestrial to the atmosphere [Barbosa et al., 2020]. It is clear that they are small enough to be carried by the wind, ocean currents, and water. Still, the specifics of how they move in and over porous media (soils, sediment, and vegetated surfaces) have seen comparatively little attention. Only six studies that investigated the transport of MPFs in porous media were found in the literature. Four of these studies looked at the infiltration in natural material (quartz sand, sand less than $2mm$, and farmland soil less than $5mm$)[Cohen and Radian, 2022, Yan et al., 2020, Han et al., 2022, Lüscher and Jo, 2022], and two used glass beads to represent soil types [Waldschläger and Schüttrumpf, 2020]; all but one of these studies were performed using a column experiment, with one using a tilting flume to capture vertical and horizontal movement [Zhang et al., 2022b].

The infiltration of MPF into porous media was investigated by Waldschläger and Schüttrumpf [2020], who performed laboratory column experiments. The study used

glass beads to represent different sediment types (fine sand, coarse sand, fine gravel, gravel, etc.) but did not include organic material analogs. Fibers had a range of infiltration depth of $2 - 110cm$, infiltration depth increased with grain size, and porosity was found to highly influences infiltration depth [Waldschläger and Schüttrumpf, 2020]. Cohen and Radian [2022] investigated the infiltration of polyester and nylon fibers in quartz sand. The length of the fiber ranged from $30 - 500\mu m$. The infiltration depth of the fiber depended on the fiber length; fibers longer than $200\mu m$ were found in the top $3cm$ of the column, and fibers shorter than $50\mu m$ were found up to $7cm$ or exited the column, it was also found that nylon type fiber infiltrated further in the column [Cohen and Radian, 2022]. A study by Han et al. [2022] looked at how fibers and film (another shape type of MPs) would impact the transport of nanoplastics (NPs) in porous media and found that fibers increase the movement of NPs by increasing the porosity and the negative attraction of the NPs and fibers. Another column study by Lüscher and Jo [2022] investigated the transport behavior of airborne MPFs in porous media using two sediment types $3mm$ glass beads and sand (the sand was tested at being layered and uniform). The run times for the experiment ranged from 24-48 hours and the lengths of the fibers were between 500 and $1000\mu m$. The results showed fibers travel a max of $16cm$ in layered sand, $24cm$ for uniform sand, and it was observed that fibers would form flocs [Lüscher and Jo, 2022].

Yan et al. [2020] looked at the vertical transport of aged (particle that have been subjected to environmental elements and under gone degradation) MPs in a loam sand column during simulated rainfall. MPFs were found to infiltrate to a depth of $9cm$ [Yan et al., 2020]. A flume study by Zhang et al. [2022b] looked at MPFs' vertical and horizontal movement during rainfall events. MPFs were found at a depth of $4-7cm$, particles in the range of $1-5mm$ stuck in the pore space, and smaller particles infiltrated further into the soil. Fibers and film had the highest mobility compared to foam and particles [Zhang et al., 2022b]. Beyond these examples, the literature on MPF reports their presence and does not consider the dynamics of their transport. Even those described here were macroscopic (upscaled) views of transport and did not consider mechanisms like sorption or trapping.

Experiments on the transport of spherical colloids have been investigated for decades. Colloid transport has used micromodels to better understand the mechanics that occur at the pore scale. Auset and Keller [2004] investigated the process dispersion on colloids of different sizes. It was found that dispersion is not only dependent on the channel structure but also the size of the colloid; larger colloids will have a lower dispersivity due to traveling in the center of the streamline and being unable to enter smaller pores [Auset and Keller, 2004]. The colloids used in the study did not allow for attachment. Zhang et al. [2015] looked at colloid attachment and remobilization due to flow rate in a micromodel with a porosity of 0.39. The flow rate

impacts the colloid attachment; the breakthrough curve data showed lower concentration than the two larger flows, and re-mobilization of the colloids only occurred at the largest flow rate [Zhang et al., 2015]. Another study on colloid transport in a saturated micromodel was performed by de Vries et al. [2022], who investigated the transport of colloids in unfavorable conditions based on Derjaguin-Landau-Verwey-Overbeek theory (DLVO). It was found that colloids could attach due to local flow velocity, and attached colloids with similar trajectories may have different behaviors (attachment, velocity, etc.) [de Vries et al., 2022].

Spherical MPs are considered colloids due to their shape. A literature review by O'Kelly et al. [2021] found twenty experimental studies investigating the transport of MPs and NPs before 2021. The size of the particles used in these studies had a range of $20nm - 5mm$, with nineteen of these studies having particles smaller than $550\mu m$ [Cai et al., 2019, Dong et al., 2018, 2019a,b, He et al., 2020, Johnson et al., 2020, Hou et al., 2020, Hu et al., 2020, Liu et al., 2019b]. O'Connor et al. [2019] performed a column study examining the vertical migration in sand soils due to wet-dry cycles. It was found that fine MPs had an infiltration depth of $7.5cm$ after twelve rain events [O'Connor et al., 2019]. A column study by Ranjan et al. [2023] looked at infiltration of MPs during simulated rainfall in sand ($0.425 - 2mm$) for the three common plastics (PE, PP, PET). The column was $47cm$ long and was broken into nine sections; PP was only present in the first section, PET was present in the second, and PE present

was found in sections three to eight [Ranjan et al., 2023]. Gui et al. [2022] looked at the dispersion and transport of MPs in three different beach sediments in a column study. The MPs used in the study had a size of 0.3, 0.5, and $1\mu m$. It was found that the larger sized MPs infiltrated further in all three soils than smaller sized MPs [Gui et al., 2022]. Another column study by Chu et al. [2019] investigated if the transfer of colloids among collectors will hold for MPs. The experiment used $1\mu m$ MPs and glass beads for the sediment, and the experiment found that MP transport behaviors agreed with the DLVO [Chu et al., 2019].

Fibers outside of porous media have been researched to understand how they move. Nagel et al. [2018] investigated the trajectories of rigid fibers with length of $211 - 614\mu m$ in a microchannel (micromodel). Fibers in transport could have three types of motions: drifting (drift from one wall to the other), pole vault (rotate over an end of the fiber) or wiggling when near the wall [Nagel et al., 2018].

There has been considerable research regarding the mobility of polymers and polymer chains. However, these are much smaller than MPFs; researchers have looked at understanding the movement and transport of elongated/fiber polymers [Schroeder, 2018, d'Angelo et al., 2010]. These flexible fibers allow them to stretch, compress, and deform by external forces. Micromodels and columns have been used to study the movement of these elastic fibers under pressure flow and gravity-driven transport [Makanga et al., 2023, Schroeder, 2018, d'Angelo et al., 2010, Calabrese et al., 2022].

Makanga et al. [2023] used a column to investigated dispersion and nontrivial trapping of flexible fiber driven by gravity. Fibers were released at the top of the water column; the fiber were observed settle to the bottom and connect with a 3D-printed object that extends the width of the column. The research found that fibers would either glide along the object or get trapped around it; these outcomes depended heavily on the mechanical and geometrical properties of the system [Makanga et al., 2023].

The simulation of polymers uses Kramer's chain, also known as the bead-rod chain. Models have been developed using this idea (e.g. [Moghani and Khomami, 2017, Edwards et al., 2018, Kim et al., 2010, Słowicka et al., 2012]). The concept is the beads are connected to the end of rods, the rods can rotate around the bead to allow the object to be flexible. Liu [1989] presented the main elements of the idea. Engdahl [2018] used a bead-rod chain to simulate the transport of MPF in porous media in a distributed simulation model. The model did not allow for elasticity, limited the rigidity of the fibers, and had no interactions between fibers nor any substrate.

The literature suggests that the dynamics of MPF transport in porous media are poorly understood. Several studies have been performed aiming to quantify MPs abundance in specific environments. However, the methods by which the MPs travel to that environment have not been elucidated. Unfortunately, this relies heavily on the infiltration rates and ignores several underlying factors such as flocculation, mechanical filtration, electrical surface interactions, etc. Additionally, many models

are meant for colloidal shapes and have not been appropriately modified for MPFs [Engdahl, 2018]. The research indicates that the transport of MPF processes between the terrestrial and aquatic systems needs to be investigated further [Akdogan and Guven, 2019]. Such an investigation would provide a better understanding of how MPFs move and where they will most likely be found, further allowing scientists to determine the risk of MPFs on the environment and humans.

1.2.4 Modeling MPFs

The transport of dissolved solutes is normally described using some variation on an advection-dispersion-equation (ADE). A common form of the ADE is

$$R\frac{\partial C}{\partial t} + \nabla \cdot vC - \nabla \cdot D\nabla C = F \tag{1.1}$$

where $C(x,t)$ is the concentration field, $F(x,t)$ is a reaction rate, $v(x,t)$ [L/T] is the vector field of velocity, R is the retardation coefficient, and $D(x,t)$ [L^2/T] is the dispersion tensor field as defined by Bear [2013]. Passive solutes can be represented by equation 1.1 when $R = 1$ and $F = 0$. Another case is when $R \neq 1$, the transport of solutes will either slow down or speed up. When $F \neq 0$, the solutes can interact with the environment, affecting the solutes' transport rate.

Reduced dimensional forms of the ADE are common in application since the full velocity field may not be known in detail. In these cases, one-dimensional forms of

equation 1.1 are used instead. A common analytical solution to the 1d ADE is

$$P(x,t) = \frac{1}{2}\text{erfc}\left(\frac{x - v^*t}{\sqrt{4D^*t}}\right) + \exp\left(\frac{x}{\alpha}\right)\text{erfc}\left(\frac{x + v^*t}{\sqrt{4D^*t}}\right) \tag{1.2}$$

where $v^* = v/R$, $D^* = (v\alpha)/R$, α is longitudinal dispersivity , P denotes the probability of arrival at location x by time t and R is the retardation coefficient for equilibrium, eversible sorption. The assumptions for (1.2) are a semi-infinite domain, a continuous source at the upstream inlet, Fickian dispersive flux, and no hydrodynamic dispersion upstream of the inlet. Reduced dimensionality forms of the ADE are often applied first to transport problems, even when some of its assumptions are not satisfied because it can still offer a first-order estimate of transport rates.

The physical characteristics of MPFs are expected to impact their motion. MPFs are unlike most other colloids and solutes because they are relatively large, discrete, non-spherical, rod-like objects that can tumble/roll and often bend. Observation of MPF movement is difficult due to their rod-like shape matching that of natural organic material like grass, roots, etc., which leads to identifying MPF nearly impossible without the use of sequential filtration or high-precision density-based separation [Eerkes-Medrano et al., 2015, Yang et al., 2021a]. These challenges likely explain why the dynamics of how MPF moves through the environment remain elusive in the literature. Since existing transport theories breakdown when considering MPF and observations/data collection are difficult, at best, physical dynamics modeling based on a balance of the forces acting on an MPF is one of the only viable options.

Engdahl [2018] created a distributed simulation model for MPF transport in porous media. The model uses a bead-rod chain to represent flexible fibers, which define the nodes where the force balance is evaluated. The chain is subjected to a constraint that its overall length cannot change, but it can deform freely, elastically, or be made nearly rigid. Simulations conducted with this model suggested that fibers that are the same or smaller than the mean pore size may behave like solutes [Engdahl, 2018], meaning that an ADE might be a reasonable approximation and that fiber length impacted transport speed. However, these hypotheses were developed entirely from simulations. No data to validate the model existed at the time, and the hypotheses regarding transport have not been verified experimentally.

1.2.5 Environmental impacts

As MPs enter the environment as primary or secondary, they can pose a potential environmental risk. The degradation of plastics in the environment can occur from mechanical breakdown, photo-, thermal-, and biodegradation. The aging and degradation of MPs will leach chemicals into the environment [Bajt, 2021, Luo et al., 2023], UV light leads to the degradation of MPF, which can also release pollutants to their surrounding environment [Shi et al., 2023]. Degradation of MPs reduces their overall size, increasing the distance particles can travel. When microplastics remain in the

soil, they can alter the structural and functional properties like the soil's pH, soil aggregation, bulk density, oxygen flow and water-holding capacity [Wang et al., 2021, Ingraffia et al., 2022, Zhou et al., 2020] and impact the vegetative and reproductive growth of plants [Yaseen et al., 2022]. As a result, this could change the relative distribution of aerobic and anaerobic microorganisms. This can potentially lead to the loss of microhabitats and, thus, the extinction of native microorganisms [Yaseen et al., 2022].

Microplastics may pose an external and internal threat to organisms. The mobility of organisms is affected when MP adheres to their body's surface, and a variety of these organisms mistake microplastics as food and ingest them due to the appealing appearance and odor of the plastics [Halfar et al., 2021, Yaseen et al., 2022]. Internal impacts can range from gastrointestinal obstruction to clogging the gills [Auta et al., 2017, Halfar et al., 2021, Huang et al., 2021], which can lead to inflammation, stress, growth, and reproduction decline [Du et al., 2021]. Shellfish and other fish species are frequently contaminated with microplastics[Yaseen et al., 2022]; research on the effects of microplastics has been conducted on mussels, crabs, fish, oysters, etc., across the globe and found reproduction, growth, and life span can be impacted. Some animals who eat microplastics, like earthworms, can move the plastics through the food chain and potentially impose MPs impacts on their predators [Yaseen et al., 2022, Lahive et al., 2022].

1.2.6 Human impacts

Microplastics are a pressing concern for public health since they are present in all environments and many products people use daily [Gambino et al., 2022, Sripada et al., 2022]. Though there is little evidence of its impact on human health, some studies have been conducted with cells in culture and other mammalian animals, like mice, upon which a risk assessment can be predicted. Evidence has been observed that humans have consumed microplastics from the bioaccumulation of seafood, plants, chickens, drinking water, and airborne microfiber fallout [Birch et al., 2020, Prata et al., 2020, Zhang et al., 2022a, Gambino et al., 2022, Yong et al., 2020, Zhang et al., 2022c]. Kosuth et al. [2018] investigated plastic pollution in tap water (globally), 12 brands of beer (around the Great Lakes) and salt (commercial). It was found that 81 percent of the tap water samples had particles and fibers made up 98 percent, each brand of salt and beer contained microplastic particles, and 99 percent of the particles were fibers [Kosuth et al., 2018]. MP contamination tends to impact wildlife organisms in one or multiple ways: digestive system, gastrointestinal, inflammation, hepatic stress, decreased growth, and decreased reproductivity and mortality. [Auta et al., 2017, Halfar et al., 2021, Huang et al., 2021, Yang et al., 2021b], it is assumed that humans could face some of these impacts and that MPs may negatively affect human health. Still, the exposures and their health implications remain either unknown

or largely un-investigated [Sripada et al., 2022].

1.3 Methodology

The research has two parts: 1.) Collecting MPF movement data and observing the transport behaviors in porous media using meso-scale experiments and MPF transport data analysis, 2.) Modeling using existing simulation tools.

1.3.1 Experimental

Micromodels or Microfluidics are used to study pore-scale processes (physical, chemical, etc.). The size of the pores is less than 1mm, and the overall size range of the model is centimeters. It has been used to study transport dynamics and flow [Karadimitriou and Hassanizadeh, 2012]. Perez et al. [2022] investigated the impact of biofilm-inducted flow in a homogeneous pore structure. The biofilm's presence leads to particles having slower breakthrough curves due to abrupt changes in the velocity and trapping events [Perez et al., 2022]. Flexible fiber colloids have been studied in micromodels to understand how they move under pressure-driven flow [Nagel et al., 2018].

One of the overall goals of this research was to visualize and capture the movement of MPF in porous media. In reviewing papers that investigated the transport of par-

ticles in porous media, the main methodology used was micromodels. This research needed to control the discharge, number of particles flowing through the model and capture the particle's movement through a desired pore structure. Micromodels give the researcher complete control of the mechanics (velocity, friction forces, etc.), can design the flow domain, and can view/capture particle transport through the domain with a camera. Given these advantages and decades of use, micromodels are a viable way to investigate the transport dynamics of MPF in porous media.

The micromodel used in this research was upscaled to understand the mechanics at a single pore. The upscaled micromodel was a 2D meso-model and has the smallest pore opening of $0.5cm$, and the overall size was $5cm$ tall, $20cm$ long, and $0.3cm$ thick domain (figure 1.2). The meso-model was chosen due to its ability to view and capture the movement of MPF through a pore structure by upscaling the environment. The model was constructed with a Markforged, Mark 2 3D printer. A poly-carbonate plate was attached to the top of the model to observe the movement of the fibers. The model was housed in an experiment rig that contained the water supply, lighting, and a camera (figure 1.3). The fiber used in this study was a neon green monofilament fishing line; while these fibers are larger than what comes off clothing, the shape and structure are the same, and these fibers are found in porous media. The pores size of the meso-model gave the ability to capture the transport dynamic in the void space. The passive solutes used were fluorescent green polyethylene microspheres

(will be referred to as beads from here on out) with a diameter size of $600 - 710\mu m$. The monofilament fishing line and fluorescent microspheres were selected due to their visibility. Increasing the fibers' visibility was done by adding two UV LED light tubes attached to the rig's side. The geometry of the meso-models was an idealized pore structure. This pore structure was chosen due to its simplicity of a homogeneous pore, and the extensive research has provided an understanding of the flow and transport physics in the porous medium [Bolster et al., 2014].

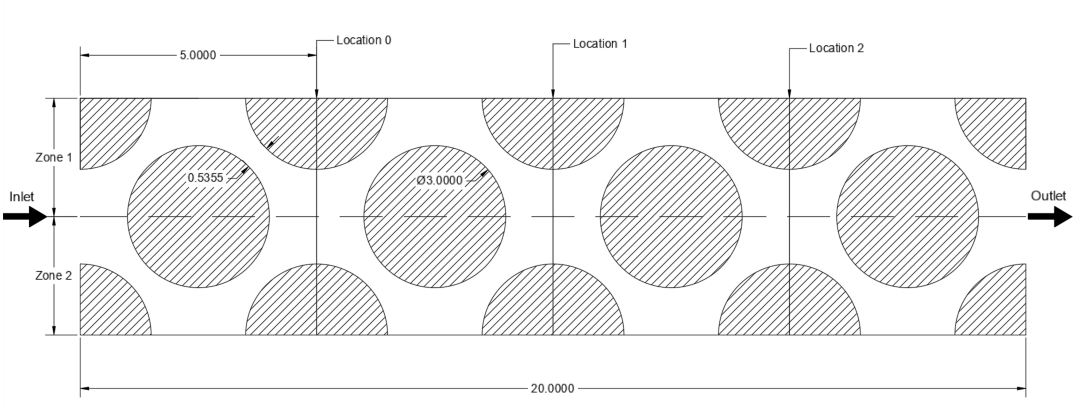

Figure 1.2: Plan view of the meso-model. All the dimensions in the figure are in centimeters. The flow will enter the model from the left and exit on the right. The middle two pores are the focus of the study.

Water flows through the meso-model from a supply tank in the upper left of the rig. A clear $0.95cm$ diameter tubing was attached to the bottom of the head tank and runs to a t-fitting attached to the meso-model, and an outlet tube was located on the right side of the model. The height difference $\Delta h = 2.3cm$ between the elevation of the water in the head tank and the outlet, this configuration generates a discharge

of $q = 4.104x10^{-6}m/s$ and a Reynolds number of $Re = 13,628.12$ for a turbulent flow through the flow domain. Without higher precision equipment, this flow rate was the lowest rate that could be sustained. The t-fitting on the inlet supply line was the injection port for the fibers and beads. A syringe was filled with water, and the particles (MPF or bead) were placed in the tip of the syringe; the syringe was attached to the t-fitting and pressed slowly until the particle entered the flow field, the open reservoir absorbed any pressure pulse from the injection of the syringe. After the prior particle moved through the model, another syringe was filled with water, and the particle was placed in the injection port. The process was repeated for 300 beads and fibers at lengths of 0.3, 0.5, and $0.8cm$ moved through the model. A single particle (fiber and beads) was investigated due to wanting to know how an individual particle transport dynamic, increasing the number of particles in the meso-model at a time would introduce dynamics between the particles like (flocculation, electrostatic interaction, etc.) that would impact the transport dynamics of the particles. The transport of the particles was captured using a GoPro Hero 7 Black, which was attached to the top of the rig and focused on the middle two pores of the meso-model. The video was recorded at 2704×1520 pixels and 30 frames per second.

The video data was subjected to a three-step process to extract the trajectory data of the fibers and passive solutes (beads): 1.) Pre-processing- A MATLAB script converts videos into frames, converts frames to binary, and enhances images by sub-

tracting background and applying noise filter functions for particle tracking software [Perez et al., 2022], 2.) Particle tracking- Fiji: A biological image analysis program, an add-on to the ImageJ, an image analysis program developed by the National Institutes of Health, was used to perform the particle tracking using the plug-in Trackmate. [Schindelin et al., 2012, Ferreira and Rasband, 2012]. The program tracked the center of mass of the particles, meaning that not all of the dynamics are being captured from the trajectories. The trajectory data does not show when the fibers are rotating, only the center mass location of the fiber traveled. , 3.) Post-processing- A MATLAB script creates a data file with all the particles' trajectories, trajectory plots, and breakthrough curves. The breakthrough curves were computed at location 1 (after the first pore) and location 2 (after the second pore) in figure 1.2 and evaluated by taking the time the particle crossed location 0 and subtracting it from the time it took the particle to cross location 1 and location 2 and the travel time is in an array for each location, this is done for each particle. The "prctile" function in MATLAB was used to make breakthrough curves; the function returns percentiles of the travel times for a percentage of $0 - 100$.

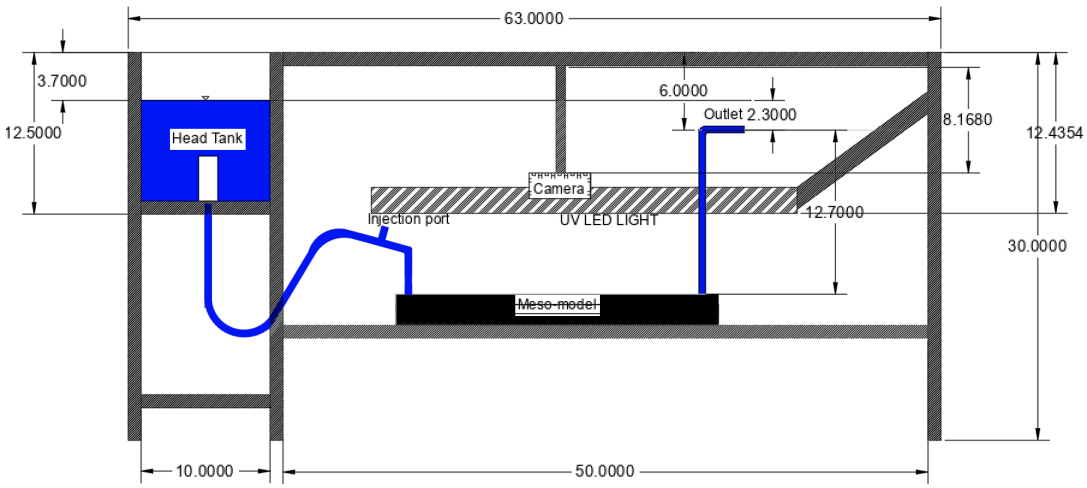

Figure 1.3: The experimental rig that houses the meso-model. The water inlet is on the left, and the outlet is on the right side of the rig. The injection point is where the syringe is connected to the supply line to introduce the fibers and beads into the flow field. All measurements are in centimeters.

1.3.2 Numerical Methods

Explict modeling

As stated in section 1.2.4, the advection-dispersion equation is the most common simulation tool. This tool is used because it is simple and widely used in solute transport. The modeling of MPF transport in porous media used existing upscaled modeling tools to fit the standard analytical solutions equation 1.2 for solute transport to the experimental breakthrough curves. The analytical solution was fit to the BTCs data by using the unconstrained non-linear optimization function "fminuc" within Matlab. "fminuc" allows for parametric approximations using robust gradient-free tools and is flexible enough also to be adapted to fitting any analytical solution to

the BTCs. The known variables in the equation 1.2 are x the position, t is the arrival time from experiment BTC, this leaves three variables to be optimized v, α and R.

Distributed simulation modeling

The objective of distributed modeling is to provide as close as possible of an analog to the laboratory experiments. In the distributed simulation, a velocity field representing the experiments was obtained by solving the Naiver-Stokes equation 1.3 and 1.4 using the add-on application FEATool (Finite Element Analysis Toolbox) in MATLAB.

$$\rho\left(\frac{\partial u}{\partial t}+(u\cdot\nabla)\,u\right)-\nabla\left(\mu\left(\nabla u+\nabla u^{T}\right)\right)+\nabla p=F \tag{1.3}$$

$$\nabla\cdot u=0 \tag{1.4}$$

where u is the velocity field, p is the pressure, $\rho = 998.2\frac{kg}{m^3}$ is the density of the fluid, $\mu = 1.002\times10^{-3}\frac{Ns}{m^2}$ is the dynamic viscosity and F is the body forces acting on the fluid. The boundary condition in the simulation was a no-slip (wall) on the top, bottom, and around the spheres. An inlet boundary condition was the average velocity in the x direction ($\bar{a} = 6.84\times10^{-2}m/s$), and the outlet boundary had a pressure of zero. The initial 2-D simulations were unable to reproduce both the velocity and the pressure drop across the domain, likely due to the friction along the walls of the model and poly-carbonate plate. The viscosity was tuned to match the pressure drop of the experiment. The simulation matched the experiment pressure

drop with a viscosity of $\mu = 4.32 \times 10^{-2} \frac{Ns}{m^2}$, suggesting significant friction resistance due to the walls of the model. The velocity field for the simulation can be seen in figure 1.4.

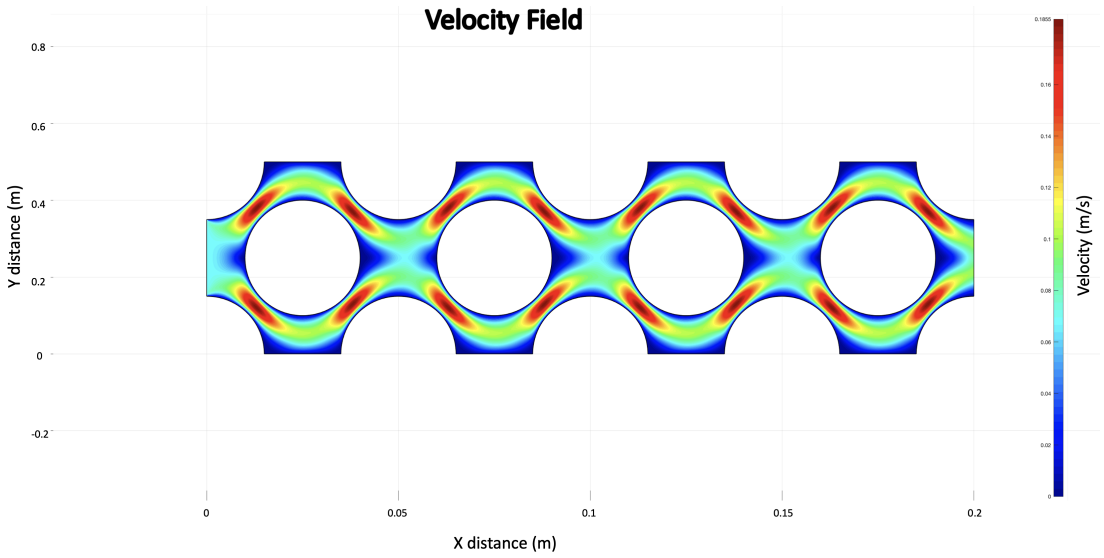

Figure 1.4: 2D simulation of the velocity field in the meso-model. The velocity of the water increases in the narrow sections and decreases in the large void spaces between pores.

1.4 Results

1.4.1 Experimental

The movement of MPF through porous media was captured during the experimental section of the project. The videos showed that MPF tends to tumble/roll through the meso-model (figure 1.5). This tumble/roll action occurred in the broad-

est part of the model and was observed at all fiber lengths. It was also observed that fibers would have an abrupt change in their velocity (fibers would slow down to a much lower velocity), become immobile, then return to being mobile or become stuck in a low-velocity zone and move in circles before re-entering a higher velocity zone. This paper will refer to this dynamic as "trapping". This trapping process may be caused by one or multiple of the following: electrostatic, vertical wedging, mechanical/hydraulic sticking behind cylinders, shear drag, etc., which will be discussed further in the following section. Most of the fibers entered the model either above or below the center line of the experiment and would stay there through the model, but fibers would switch between between above and below the center line after the first pore. The zone switching occurred for all fiber lengths. 3mm fibers had the most zone switches, and the occurrence decreased with the increase of fiber length (figure 1.6). The passive tracers (beads) also tended to switch zones after the first pore. The trajectory paths of the beads are less dispersed than fibers (figure 1.6). Figure 1.7 shows the BTCs of the fibers and beads for the first and second pores.

1.4.2 Numerical Methods

Explict modeling

The analytical solution of the ADE equation 1.2 was fit to the experimental BTCs for all fibers and beads as they passed the end of pore 1. The ADE equation effectively

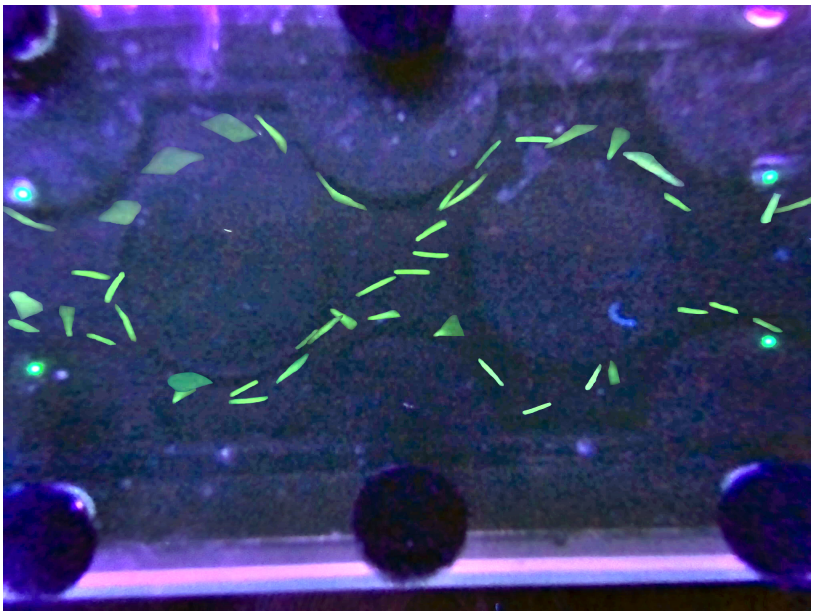

Figure 1.5: This figure is a composite of three different fibers multiple times through the meso-model. This composite provides a visual demonstration of the experimental results. One fiber travels above both pores, another travels below both pores, and the last fiber travels below the first and above the second pore. Each fiber tumbles/rolls in large pore openings.

captured the middle section of the BTCs for the beads but was unable to capture the tail and the front of the BTCs. However, the overall description is reasonably good (figure 1.8.a). The fits for the fiber were not as robust as the beads; the ADE predicts fibers moving faster than the experiment at the front of the curves. Given the velocity and dispersion coefficient decoupled from the known velocity, the central portion of the breakthrough curves could be captured. The simulated values for the ADE equation are found in table 1.1 and show that v decreases with an increase in particle size and α increases by a factor of ten from beads to fibers. At the same time, the fits are decent but they are completely disconnected from reality due to

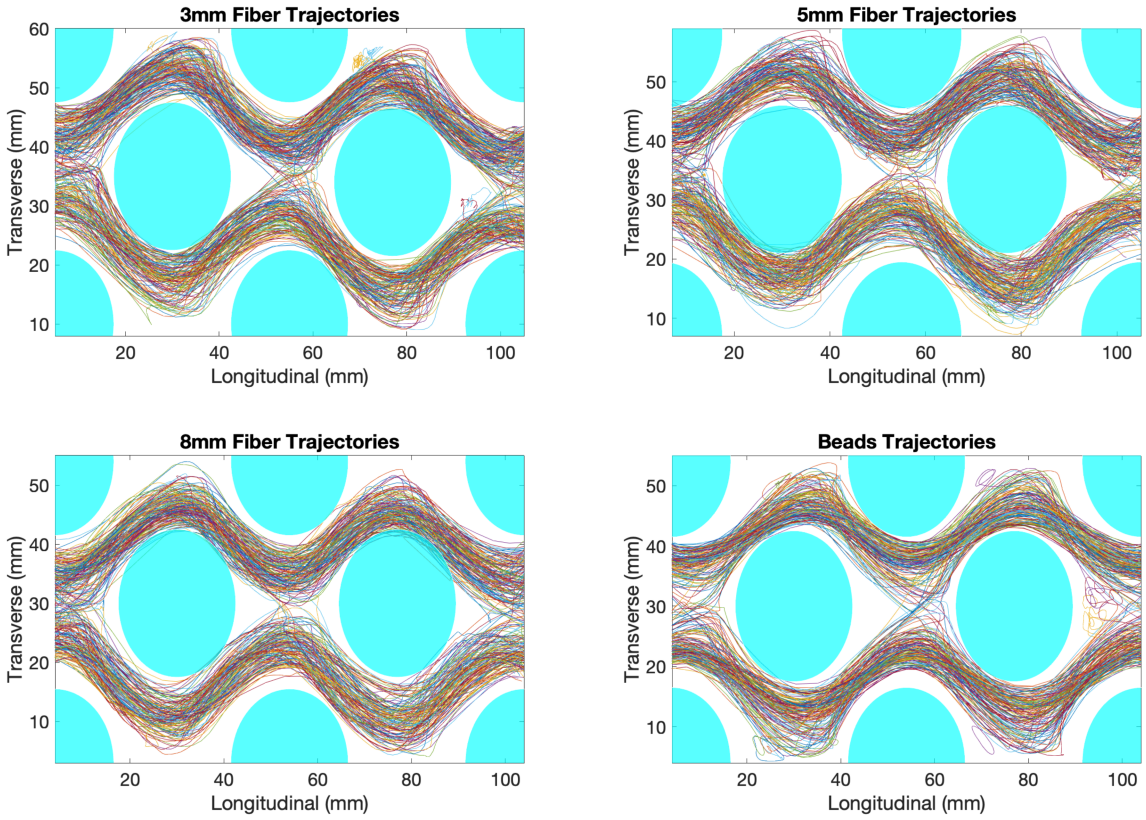

Figure 1.6: This figure shows the trajectories of 300 particles for each fiber length and beads. These trajectories show that fibers and beads will switch travel zones between pores; the occurrence decreases with the increase in fiber length. The beads' trajectories are in a thinner band than the fibers, subjecting them to the velocity field's faster section.

how different the speeds are from the beads.

Distributed Simulation Modeling Validation

The results from the ADE fits show that a more robust model like the distributed simulation model is needed for modeling MPF transport. The transport of the beads was able to be accurately simulated in the distributed simulation model (DSM). The simulation (fiber-sim) predicted that fibers of any length should be moving at speeds

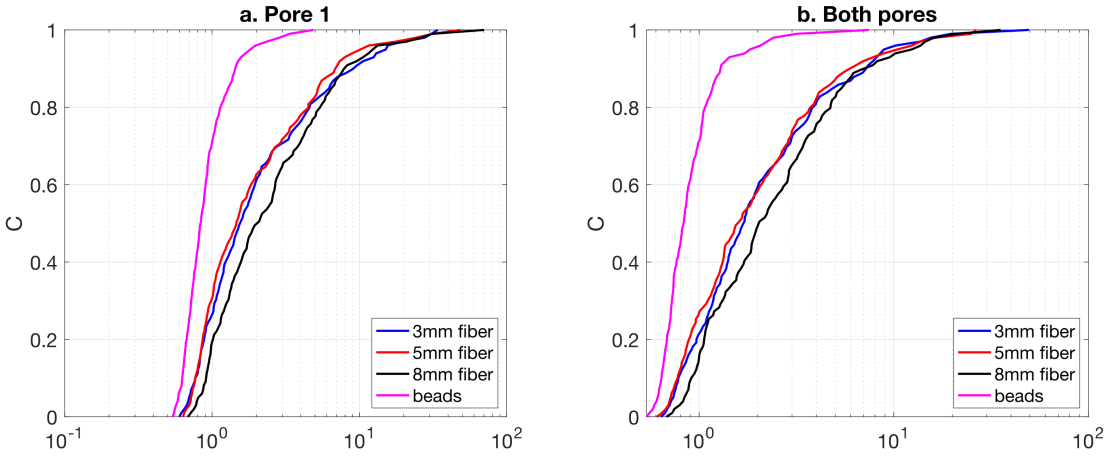

Figure 1.7: These graphs show the BTC for pore one and both pores. The BTCs are normalized by the mean breakthrough time for the beads. Fibers move slower than beads. 8mm length fibers are the slowest moving fibers; 3 mm and 5mm fibers have similar travel times.

very similar to the beads (figure 1.8.b), but this is not the case in the experiments (solid lines). The question is why do they disagree and what can be done to improve the simulation.

Preliminary work by Nick Engdahl constructed two modified DSMs to account for the trapping process dynamic missing from the original distributed simulation model. The first modified model (WT) has a waiting time that is exponentially inverse proportional to the velocity critical threshold in which there is no trapping, which only has one free parameter, and the second model (Trap) uses a waiting time distribution. The following two sections discuss each model and the results.

DSM with waiting time

The transport of solutes, colloids, fibers, etc., interacts with the environment, which can alter the travel time of the particle. The interaction between the envi-

ronment and the particles can be due to electrostatic forces, diffusion, sorption, or being subjected to low-velocity zones in the flow field, leading to late arrival on the BTCs. It has been established that the late arrivals in the BTCs are essential to understanding and modeling environmental contaminant movement. Models have been developed for decades to understand and capture these late-time arrivals [Baeumer et al., 2001, Margolin et al., 2003, Patrick Wang et al., 2005].

One method to capture the interaction of solutes with their surrounding environment (diffusion, linear non/equilibrium sorption) is the subordinated process that describes the particle's movement from mobile to immobile (equation 1.5)

$$q(x,t) = \int_0^\infty a(x,u)\, h(u,t)\, du \tag{1.5}$$

where $q(x,t)$ is the density, $a(x,u)$ is the linear time model for particles motion, $h(u,t)$ adjust the particles that are mobile [Benson and Meerschaert, 2009]. The gamma distribution in MATLAB was used to generate a PDF for each fiber length (equation 1.6), and equation 1.7 is the gamma function. The gamma distribution solves for two unknowns ϵ and β, where ϵ is the shape parameter and β is the scale parameter.

$$y = \frac{1}{\beta^{\epsilon}\Gamma(\epsilon)} x^{\epsilon-1} e^{\frac{-x}{\beta}} \tag{1.6}$$

$$\Gamma(x) = \int_0^\infty e^{-t} t^{x-1} dt \tag{1.7}$$

The optimization function "fmincon" in MATLAB was used to find the best-fit values for the unknown variables of the gamma distribution (ϵ and β) for each fiber length. The gamma distribution values are in Table 1.2 for all fibers. The results of the upscaled model using the waiting time (WT) can closely capture the experimental (Exp) BTCs seen in figure 1.8.c.

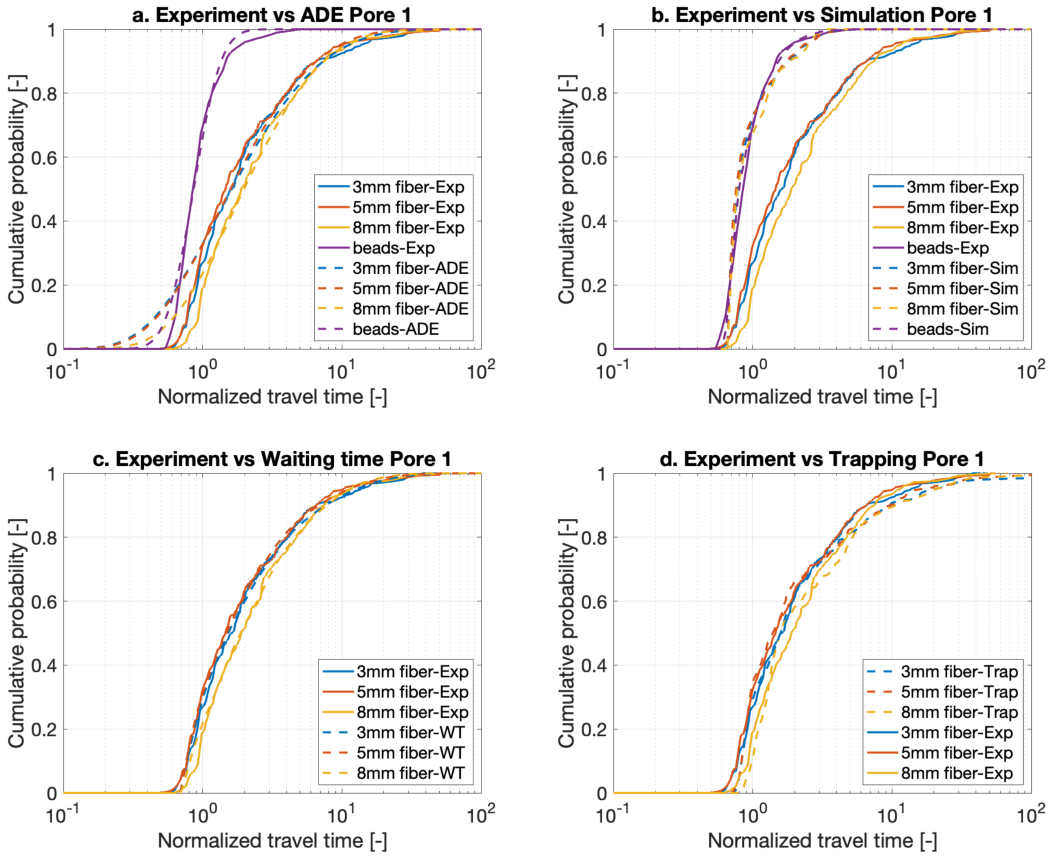

Figure 1.8: These figures show the BTCs for the four models used to simulate MPF transport. The ADE simulation (a) can capture the middle of the beads and the last 0.7 of the fiber curves but has beads and fibers moving faster than the experiments at the front of the curves and the tail for the beads. The distributed simulation model (b) does a very good job of simulating the transport of beads, but the simulation had fibers with a similar arrival time as the experimental beads. The simulation can capture the dynamic of $3mm$ and $5mm$ fibers having similar travel times and $8mm$ fibers traveling slower. The distributed simulation model with waiting time (c) produces BTCs similar to the experiments. The distributed simulation model with trapping (d) has similar BTCs as the experiments tell 0.8; trapping starts to over-predict and has a slower arrival time for all fibers.

DSM with Trapping

As stated above, particles interact with the environment in several ways, leading to slower BTCs. Since it has already been established that a waiting time provides a good upscale description of the behaviors relative to the original model, this suggests that something having a nearly exponential waiting time distribution is causing the lag, which could be a result of electrostatic friction, low-velocity zones, the interaction between the meso-model or abrupt change in the velocity of the particle. To provide a better understanding of which of these factors are causing this "trapping process," the experiment can be repeated using a different type of material to make the meso-model remove surface and electrostatic friction. A simple and fast way to account for the "trapping process" is to modify the DSM to account for trapping.

The distribution of waiting times is represented as an exponential distribution where the probabilities are proportionate to the time step and the inverse of the velocity, and the only fitting parameter is a critical velocity above which trapping does not occur. A waiting time does not affect the trajectory of the fibers, so this model can be applied without re-running the entire simulation, making it simple to apply and calibrate the threshold velocity. Waiting times at each step along the trajectory were simulated as independent random variables, and the waiting time was added to the time for that step along the trajectory.

The trapping process added to the DSM does a good job at capturing the transport

of MPFs (figure 1.8.d), but the simulation starts to overpredict the trapping process at the tail of the curves. The simulation has $8mm$ fibers moving slower than the $3mm$ and $5mm$ fibers. The $3mm$ and $5mm$ fibers have similar breakthrough curves, as seen in the experimental results.

1.5 Discussion

1.5.1 Experiments

The observation of MPF transport provided the information that MPFs move as a rigid rotor that tumbles/rolls in large void spaces. Figure 1.5 is a composite of three fiber trajectories through the model that shows the tumble/roll dynamic of the fibers in the large void spaces; fibers are a straight ridged line that will move above/below both pores or switch from the bottom of one pore to the top of the other (or vice versa). Most MPF will travel through the model above or below both pores, but some fibers would switch from above to below or vice versa in between the pores. This dynamic occurred for all fiber lengths but was more prevalent in the shorter fibers (figure 1.6). The beads had the same transport dynamics of switching from above to below or vice versa. The videos also showed that fibers could experience abrupt changes in the transport velocity, while the beads did not; this suggest the MPFs were interacting with the meso-model. Examining the trajectory plots (figure

1.6) of the simulated velocity field (figure 1.4), it can be seen that all fiber lengths are subjected to a wide range of velocities. Analysis of the trajectory data confirmed that fibers would have slower arrival times than beads, and shorter-length fibers will travel faster than longer fibers (figure 1.7). Fibers with a length of 3 and $5mm$ have very similar BTCs; this suggests that fibers equal to or less than the smallest pore opening (SPO) will have a comparable arrival time. Lengths longer than the SPO will have slower travel times, and the longer the fiber, the slower it will travel (figure 1.7).

The key contribution of this research is the capturing of MPFs trajectories for the first time and these experiments had two main findings: 1.) Fibers will move slower than spherical colloids, and 2.) Fiber lengths impact travel times. These findings have been established in studies that focused on the infiltration rate of MPs [O'Connor et al., 2019, Zhang et al., 2022b]. Waldschläger and Schüttrumpf [2020] stated that MP spheres infiltrated further in different simulated classes of sediment (glass spheres); the assumption can be made that spheres travel faster, which corresponds to the finding in this research. As to the impact of fiber length on the infiltration rates Cohen and Radian [2022] found that shorter fibers will travel further in the column compared to longer fibers. The longer fibers enter an immobile zone (become stuck), which corresponds to these fibers traveling slower, as seen in the experimental BTCs (figure 1.7).

1.5.2 ADE

Modeling MPF transport was unable to be done with the ADE equation 1.2. The ADE simulation has bead particles moving faster than the experimental from $0-0.25$ of the BTC, and the last 20 percent (tail) of the ADE BTCs also moves faster than the experimental BTC. Looking at the results of the ADE simulation on the fibers, the ADE can closely simulate the last 75 percent of the BTCs for all fiber lengths. In this section, the ADE can produce the same dynamics in the curves as in the experiment; there is little difference between the $3mm$ and $5mm$ fibers, and $8mm$ fibers move slower than the two shorter fibers. The ADE simulation cannot capture the front of BTCs for any fiber length; fibers are moving faster than the experimental curves (figure 1.8.a). The simulated values for the ADE equation are found in table 1.1 and show that v decreases with an increase in particle size; there is a slight increase in v for $5mm$ fibers. α increases by a factor of ten from beads to fibers and decreases when the fibers' length increases. This trend indicates dispersivity is dependent on the particle size, Auset and Keller [2004] had the same trend in their colloid transport research.

Best fit ADE simulation values				
Particle	3mm fiber	5mm fiber	8mm fiber	Beads
v	0.0263	0.0290	0.0250	0.0898
α	0.0493	0.0417	0.0348	0.0033
R	1	1	1	1

Table 1.1: Best fit values of ADE simulation for all particles for pore 1

1.5.3 Distributed simulation model

The distributed simulation model (DSM) can simulate the movement of beads; figure 1.8.b shows the bead simulation (purple dashed lines) closely follows the BTCs of the experiments. It can be seen in figure 1.8.b that the fiber simulation in the DSM was faster than the experiments; this indicates the velocity field does not represent the fiber's velocity. Focusing on the simulation results of all the particles, the BTCs will have a similar arrival time for the first 70 percent of the curve, with fibers having a slightly faster arrival. Above the 70 percent mark, fibers start to have a slower travel time. The DSM can capture the dynamic of longer fibers that will travel slowly, as seen in the experimental BTCs. The fibers in the DSM are deforming (being bent in half) to move through the model, which subjects the fibers to only interact with the faster velocity field and bypass any interaction with the slower section of the velocity

field. In contrast, fibers interact with a more significant portion of the velocity field in the experiment.

Another dynamic not captured in the simulation is fibers switching zones between pores; in the experiment trajectories, all particle sizes had this dynamic (figure 1.6). This zone-switching dynamic influences the BTCs by subjecting particles to low-velocity zones in the large void space between pores, resulting in slower travel times. The generated flow field may not fully capture the experiment flow field in the meso-model. The experiment flow may be turbulent, and the simulation treats it as a laminar flow. The roughness of the meso-model can impact the flow and the transport of the fibers in the meso-model; roughness affects the friction, which will change the flow type (laminar, turbulent, and transition). The rough surface of the model can lead to particle ends getting wedged between the model surface and the poly-carbonate face plate. This can lead to particles becoming stuck or slowing down, leading to slower arrival times.

Overall, the primary dynamic the DSM is missing is called the "trapping process" the fibers experience in their transport through the meso-model. This trapping process can be caused by many factors, including abrupt changes in velocity, electrostatic attraction, fiber ends interacting with the surface of the meso-model, fibers subjected to low-velocity zones (advective trapping), etc. Research has focused on identifying the trapping of solutes during transport and what simulation tools can model this

process [Hidalgo et al., 2022, Ben-Noah et al., 2023, Talon et al., 2023]. Hidalgo et al. [2021] looked at advective trapping in homogeneous and heterogeneous media and found that a continuous time random walk (CTRW) could simulate the BTC from the experiments. The CTRW must account for either the trapping rate or trapping time distribution.

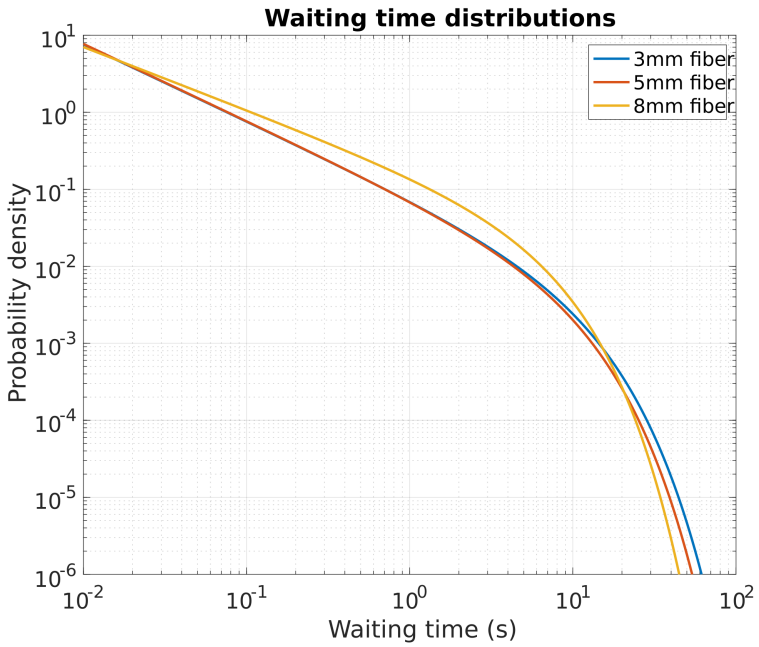

Figure 1.9: This figure shows the waiting time distribution for each fiber length. The $8mm$ fibers jump in the middle of the curve while the 3 and $5mm$ stay the same.

Applying the waiting time (WT) to the DSM does a significant job at capturing the transport of MPFs seen in figure 1.8.c. This method can capture the tail of the experiments and also does an significant job of capturing the leading edge of the breakthrough curves. The original DSM and WT have similar leading edges but the

DSM waiting time simulation values			
Particle	3mm	5mm	8mm
ϵ	$7.56 * 10^-6$	$1.73 * 10^-6$	0.183
β	8.629	7.403	5.041

Table 1.2: Gamma values for DSM waiting time simulation for all particles for pore 1

WT follow the experimental BTCs, while the DSM has faster travel times. The ADE has similar BTCs to the WT from $0.2 - 1$. The front of the ADE simulation exhibited faster travel times than the WT BTCs. The WT model would be a better choice over the ADE and DSM due to how well it captures the experimental BTCs (figure 1.8). The parameters of the gamma distribution are found in table 1.2 and shows that both ϵ and β depend on the particle size, ϵ increase, and β decrease with the increase in particle size, but the mean gamma distributions decrease with the increase in fiber length. The waiting time distribution for each fiber is plotted in figure 1.9, which shows that $8mm$ fibers have a big jump in the middle of the curve, and the other fibers stay constant.

The second modified DSM with trapping (Trap) can overall closely simulate the experiment (Exp) BTCs (figure 1.8.d). Looking at the $3mm$ and $5mm$ fibers, the Trap has particles arriving slower at the front of the curve, but the simulation following the Exp from $0.1 - 0.75$, where the trapping starts to predict over trapping which

results in a slower arrival time from $0.75 - 1$. In the $8mm$ fibers, the simulation does an significant job of capturing the front of the curve. Still, at about $0.4 - 0.65$, the Trap has particles moving faster than the Exp, and above 0.65, the models start to over-predict trapping, resulting in particles moving slower than the experimental BTCs (figure 1.8.d).

Comparing the Trap simulation to the other models is seen in figure 1.8. The Trap and ADE simulations have similar BTCs for $0.3 - 0.8$. The trapping model over-predicts above 0.8, producing a slower travel time than the ADE. The ADE simulation reasonably captured the tail of the experimental BTCs (figure 1.8). Applying trapping to the DSM model produced BTCs that have slower travel times than the original DSM for fibers (figure 1.8), the fronts of the curves are reasonably close to each other, the distance between them grows larger with increasing travel time. The trapping simulation allows the fiber to become trapped, while the DSM did not account for this transport dynamic. Knowing that the original DSM model was unable to simulate the transport of MPF, a waiting time was added to the model. Comparing the DSM-WT to the DSM-Trap simulation, the BTCs generated are very similar to each other by 0.85, and then the trap simulation produces slower travel times for all fiber lengths (figure 1.8). Both models were able to simulate the transport of MPF; DSM-WT out preforms due to its flexibility but DSM-Trap dues a good job considering how simple it is.

1.5.4 Research limitations

The two main categories of limitations of the research that should be considered are the material of the fibers and the meso-model. The following paragraphs will expand on how these two things are a limitation of this research.

The monofilament fishing line is a limitation of this research due to the size of the material. Fibers from textiles are significantly smaller in diameter than the fishing line. The larger diameter impacts the rigidity of the fiber; shorter-length fibers will be more rigid than longer fibers. Further research must determine how much the rigidity changes with length. Textile fibers with a smaller diameter will be less rigid, allowing fibers to deform. This deformation of the fibers may decrease the travel time because fibers can bend around pores and become stuck.

The meso-model is the second limitation in this research due to the print quality and the model's overall size. The quality of the print controls the roughness of the model's surface, which impacts the velocity of water and the transport of the particles. The model's surface was not modified after printing, so the rough surface increases the friction forces acting on the water. This rough surface can lead to fibers being wedged between a ridge of the surface and the poly-carbonate top plate, which will impact the travel times. The model is a pseudo 2d flow and 3d modeling of the flow field was not done. The size is a limitation due to upscaling the process of MPF

moving in porous media from a small scale of millimeters to a pore in centimeters.

1.6 Development of this project

This research project was the final product of three other research plans. The following section will discuss the other research plans and the development of the methods used in this research.

At the beginning of this project, only two publications had investigated the transport of MPF in porous media. These studies were column studies that used glass spheres to represent sediment. The results of these two studies provided infiltration data of MPF in simulated sediment. This led us to our first plan of conducting a column study that investigated the infiltration of MPF in natural sediment material. The column used in the study was a square column with an area of $103cm^2$ and a length of $31cm$, and the material used had a porosity of $\phi = 0.40$. The textile MPF from fleece was used in the study. The MPF was obtained from rubbing/washing the fleece in four liters of water to get our MPF solution; the concentration of MPF solution was determined by pouring $500mL$ over a $200\mu m$ filter and weighing the mass of the fibers. The methodology of the experiment was to pour a known volume of the MPF solution into the top of the column at a constant rate when all of the water passed through the column section of the column was removed and placed in a device

that separates MPF by elutriation/flotation. The idea of the device was developed by Claessens et al. [2013]. A PVC column with air and water injected in the bottom disturbs the sediment, and lighter particles rise to the top of the water column. The water exits the column and flows over a $200\mu m$ filter. The problem with this methodology was fine sediment particles and debris clogged the filters, and quantifying MPF was very difficult. To quantify MPF, we needed a more robust methodology.

The second research plan investigated how MPF moves at the pore scale. Engdahl [2018] developed a distributed simulation on the movement of MPF in porous media. This model is physics-based and had not been validated by any data at the time. Our plan was to collect transport data to validate the model. The method chosen to collect the data was a micromodel because this methodology has been used for decades to study transport dynamics, colloid transport, two-phase flow, etc. The problem with the micromodel was one of size; either the model was too small or MPF too big. The third research plan was to scale the micromodel from mm scale to cm scale. The first model was a single periodic pore that was $10cm$ by $10cm$ and made of layered poly-carbonate. The concept of the idea worked, and fiber transport could be observed through the model. The problem with the design was boundary effects at the inlet and outlet and fiber getting stuck at the inlet. To overcome these problems, the model was modified to have four periodic pores in a row were constructed. The model design was used in this research project.

The final step in developing the methodology used in this research was a trial and error process. The first obstacle was finding a fiber material that would be visible. UV lights were used in the experiment to help increase the visibility of the fibers. Two types of material were tested: 1) cotton thread- this material was white and could barely seen flowing through the model. 2.) Monofilament fishing line- this material was a fluorescent neon green color and was very visible during the movement through the model. The next step was to develop the injection of the fiber into the flow field. A syringe was used to inject the fibers, but the location of the fiber in the syringe impacted if the fiber entered the flow field—fibers needed to be in the tip of the syringe for easy injection. The number of fibers injected in the model was reduced to one because fibers interact with each other and impact their transport, but multiple fibers in close proximity also made image tracking difficult. This injection step was repeated for the passive tracer test (beads). It was found that beads would also interact with each other and impact their transport, so only one bead was injected at a time. The final part of the methodology was capturing the trajectories and exporting the data. A GoPro camera was used to capture the middle two pores; the camera ran continuously during the experiment. The video was broken into shorter videos of a single particle moving through the model. A MATLAB script (image processing) was developed to convert the video into frames, convert them to binary, and filter images (background subtraction and noise filtering). The image sequences

were imported in Fiji to extract the particle's trajectory, which had to be done for one particle at a time (repeated 1200 times). The trajectory data was imported in MATLAB and stored as a data file.

The developed methodology used in research is as follows: monofilament fishing and fluorescent microbeads were used due to their visibility, DI water was used to reduce cloudy film on the poly-carbonate top plate, one particle was placed in the syringe tip for injection (repeated 1200 times for all particles), extract individual particle transport videos from the longer videos, run the image processing script in MATLAB, extract the trajectory data using Fiji for each particle individually, run MATLAB script to import trajectory data for analysis. The most time-consuming part of this research was injecting 1200 particles into the model and extracting the trajectory data.

1.7 Conclusions

This paper has provided the first visual and trajectory data set of microplastic fiber transport in porous media. The trajectory data analysis found that MPFs travel slower than beads, and fibers of shorter lengths travel faster. The key takeaway from the optical data is that fibers move as a ridged rotors, tumble/roll in large void spaces, and travel above the first pore and then below the second or vice versa. In porous

media, it has been observed that MPFs have a tendency not to exhibit continuous motion.

The ADE equation is unable to represent MPF transport; overall, it is not a robust model and is too simple. This simulation method cannot capture the front and tail of the experiment BTCs. The comparison to direct simulations highlights the potential role of trapping processes, which will likely need to be addressed in more detail to develop predictive models of fiber mobility. The most accurate description involved a waiting time, which suggested the possibility of an exponentially distributed waiting time process. The specific mechanisms affecting transport cannot be assessed from these experiments, and new ones will need to be designed to better understand the factors affecting fiber transport in porous media, but it is clear some retention is occurring.

The original distributed simulation model could simulate the transport of beads from the experiment but was unable to simulate the transport of the fibers. The central dynamic missing from DSM is a "trapping process"; once the correction to the model was made, the DSM did a significant job simulating the transport of MPFs in porous media.

However, this research is only the start of understanding the transport dynamics of MPF in porous media. Further studies are needed to fully understand other factors like types of fibers, whether a heterogeneous pore structure changes MPF transport

dynamics, and how changing discharges will impact transport. Overall, the complexity of the experiment design can be increased to further the understanding of MPF transport dynamics, specifically the mechanisms causing trapping and retention of MPFs.

BIBLIOGRAPHY

Akdogan, Z. and Guven, B. (2019). Microplastics in the environment: A critical review of current understanding and identification of future research needs. *Environmental Pollution*, 254:113011.

Alimi, O. S., Farner Budarz, J., Hernandez, L. M., and Tufenkji, N. (2018). Microplastics and nanoplastics in aquatic environments: Aggregation, deposition, and enhanced contaminant transport. *Environmental science & technology*, 52(4):1704–1724.

Alipour, S., Hashemi, S. H., and Alavian Petroody, S. S. (2021). Release of microplastic fibers from carpet-washing workshops wastewater. *Journal of Water and Wastewater; Ab va Fazilab (in persian)*, 31(6):27–33.

Alvim, C. B., Mendoza-Roca, J. A., and Bes-Piá, A. (2020). Wastewater treatment plant as microplastics release source – Quantification and identification techniques. *Journal of Environmental Management*, 255:109739.

Andrady, A. L. (2011). Microplastics in the marine environment. *Marine Pollution Bulletin*, 62(8):1596–1605.

Athey, S. N., Adams, J. K., Erdle, L. M., Jantunen, L. M., Helm, P. A., Finkelstein, S. A., and Diamond, M. L. (2020). The widespread environmental footprint of

indigo denim microfibers from blue jeans. *Environmental Science & Technology Letters*, 7(11):840–847.

Auset, M. and Keller, A. A. (2004). Pore-scale processes that control dispersion of colloids in saturated porous media. *Water resources research*, 40(3).

Auta, H. S., Emenike, C. U., and Fauziah, S. H. (2017). Distribution and importance of microplastics in the marine environment: A review of the sources, fate, effects, and potential solutions. *Environment International*, 102:165–176.

Baeumer, B., Benson, D. A., Meerschaert, M. M., and Wheatcraft, S. W. (2001). Subordinated advection-dispersion equation for contaminant transport. *Water Resources Research*, 37(6):1543–1550.

Bajt, O. (2021). From plastics to microplastics and organisms. *FEBS Open Bio*, 11(4):954–966.

Barbosa, F., Adeyemi, J. A., Bocato, M. Z., Comas, A., and Campiglia, A. (2020). A critical viewpoint on current issues, limitations, and future research needs on micro-and nanoplastic studies: From the detection to the toxicological assessment. *Environmental Research*, 182:109089.

Bear, J. (2013). *Dynamics of Fluids in Porous Media*. Courier Corporation.

Ben-Noah, I., Hidalgo, J. J., Jimenez-Martinez, J., and Dentz, M. (2023). Solute

Trapping and the Mechanisms of Non-Fickian Transport in Partially Saturated Porous Media. *Water Resources Research*, 59(2):e2022WR033613.

Benson, D. A. and Meerschaert, M. M. (2009). A simple and efficient random walk solution of multi-rate mobile/immobile mass transport equations. *Advances in Water Resources*, 32(4):532–539.

Birch, Q. T., Potter, P. M., Pinto, P. X., Dionysiou, D. D., and Al-Abed, S. R. (2020). Sources, transport, measurement and impact of nano and microplastics in urban watersheds. *Reviews in Environmental Science and Bio-Technology*, 19(2):275–336.

Blettler, M. C. M., Abrial, E., Khan, F. R., Sivri, N., and Espinola, L. A. (2018). Freshwater plastic pollution: Recognizing research biases and identifying knowledge gaps. *Water Research*, 143:416–424.

Bolster, D., Méheust, Y., Le Borgne, T., Bouquain, J., and Davy, P. (2014). Modeling preasymptotic transport in flows with significant inertial and trapping effects–the importance of velocity correlations and a spatial Markov model. *Advances in water resources*, 70:89–103.

Boyle, K. and Örmeci, B. (2020). Microplastics and Nanoplastics in the Freshwater and Terrestrial Environment: A Review. *Water*, 12(9).

Cai, L., He, L., Peng, S., Li, M., and Tong, M. (2019). Influence of titanium diox-

ide nanoparticles on the transport and deposition of microplastics in quartz sand. *Environmental Pollution*, 253:351–357.

Calabrese, V., Gyorgy, C., Haward, S. J., Neal, T. J., Armes, S. P., and Shen, A. Q. (2022). Microstructural dynamics and rheology of worm-like diblock copolymer nanoparticle dispersions under a simple shear and a planar extensional flow. *Macromolecules*, 55(22):10031–10042.

Carr, S. A., Liu, J., and Tesoro, A. G. (2016). Transport and fate of microplastic particles in wastewater treatment plants. *Water Research*, 91:174–182.

Chae, Y. and An, Y.-J. (2018). Current research trends on plastic pollution and ecological impacts on the soil ecosystem: A review. *Environmental pollution*, 240:387–395.

Chu, X., Li, T., Li, Z., Yan, A., and Shen, C. (2019). Transport of Microplastic Particles in Saturated Porous Media. *Water*, 11(12):2474.

Claessens, M., Van Cauwenberghe, L., Vandegehuchte, M. B., and Janssen, C. R. (2013). New techniques for the detection of microplastics in sediments and field collected organisms. *Marine pollution bulletin*, 70(1-2):227–233.

Cohen, N. and Radian, A. (2022). Microplastic Textile Fibers Accumulate in Sand

and Are Potential Sources of Micro (nano) plastic Pollution. *Environmental Science & Technology*, 56(24):17635–17642.

Corapcioglu, M. Y. and Fedirchuk, P. (1999). Glass bead micromodel study of solute transport. *Journal of contaminant hydrology*, 36(3-4):209–230.

d'Ambrières, W. (2019). Plastics recycling worldwide: Current overview and desirable changes. *Field Actions Science Reports. The journal of field actions*, (Special Issue 19):12–21.

d'Angelo, M. V., Semin, B., Picard, G., Poitzsch, ME., Hulin, J.-P., and Auradou, H. (2010). Single fiber transport in a fracture slit: Influence of the wall roughness and of the fiber flexibility. *Transport in porous media*, 84:389–408.

De Falco, F., Cocca, M., Avella, M., and Thompson, R. C. (2020). Microfiber release to water, via laundering, and to air, via everyday use: A comparison between polyester clothing with differing textile parameters. *Environmental science & technology*, 54(6):3288–3296.

de Vries, E. T., Tang, Q., Faez, S., and Raoof, A. (2022). Fluid flow and colloid transport experiment in single-porosity sample; tracking of colloid transport behavior in a saturated micromodel. *Advances in Water Resources*, 159:104086.

Ding, R., Tong, L., and Zhang, W. (2021). Microplastics in Freshwater Environments: Sources, Fates and Toxicity. *Water Air and Soil Pollution*, 232(5):181.

Dodson, G. Z., Shotorban, A. K., Hatcher, P. G., Waggoner, D. C., Ghosal, S., and Noffke, N. (2020). Microplastic fragment and fiber contamination of beach sediments from selected sites in Virginia and North Carolina, USA. *Marine Pollution Bulletin*, 151:110869.

Dong, Z., Qiu, Y., Zhang, W., Yang, Z., and Wei, L. (2018). Size-dependent transport and retention of micron-sized plastic spheres in natural sand saturated with seawater. *Water research*, 143:518–526.

Dong, Z., Zhang, W., Qiu, Y., Yang, Z., Wang, J., and Zhang, Y. (2019a). Co-transport of nanoplastics (NPs) with fullerene (C60) in saturated sand: Effect of NPs/C60 ratio and seawater salinity. *Water research*, 148:469–478.

Dong, Z., Zhu, L., Zhang, W., Huang, R., Lv, X., Jing, X., Yang, Z., Wang, J., and Qiu, Y. (2019b). Role of surface functionalities of nanoplastics on their transport in seawater-saturated sea sand. *Environmental Pollution*, 255(1):113177.

Du, H., Xie, Y., and Wang, J. (2021). Microplastic degradation methods and corresponding degradation mechanism: Research status and future perspectives. *Journal of Hazardous Materials*, 418:126377.

Edwards, C. N., Sefiddashti, M. H. N., Edwards, B. J., and Khomami, B. (2018). In-plane and out-of-plane rotational motion of individual chain molecules in steady shear flow of polymer melts and solutions. *Journal of Molecular Graphics and Modelling*, 81:184–196.

Eerkes-Medrano, D., Thompson, R. C., and Aldridge, D. C. (2015). Microplastics in freshwater systems: A review of the emerging threats, identification of knowledge gaps and prioritisation of research needs. *Water research*, 75:63–82.

Engdahl, N. B. (2018). Simulating the mobility of micro-plastics and other fiber-like objects in saturated porous media using constrained random walks. *Advances in Water Resources*, 121:277–284.

Ferreira, T. and Rasband, W. (2012). ImageJ user guide. *ImageJ/Fiji*, 1:155–161.

Gambino, I., Bagordo, F., Grassi, T., Panico, A., and De Donno, A. (2022). Occurrence of Microplastics in Tap and Bottled Water: Current Knowledge. *International Journal of Environmental Research and Public Health*, 19(9):5283.

Gaylarde, C., Baptista-Neto, J. A., and da Fonseca, E. M. (2021). Plastic microfibre pollution: How important is clothes' laundering? *HELIYON*, 7(5).

Ghayebzadeh, M., Taghipour, H., and Aslani, H. (2021). Abundance and distribu-

tion of microplastics in the sediments of the estuary of seventeen rivers: Caspian southern coasts. *Marine Pollution Bulletin*, 164:112044.

Gui, X., Ren, Z., Xu, X., Chen, X., Chen, M., Wei, Y., Zhao, L., Qiu, H., Gao, B., and Cao, X. (2022). Dispersion and transport of microplastics in three water-saturated coastal soils. *Journal of Hazardous Materials*, 424:127614.

Halfar, J., Brozova, K., Cabanova, K., Heviankova, S., Kasparkova, A., and Olsovska, E. (2021). Disparities in Methods Used to Determine Microplastics in the Aquatic Environment: A Review of Legislation, Sampling Process and Instrumental Analysis. *INTERNATIONAL JOURNAL OF ENVIRONMENTAL RESEARCH AND PUBLIC HEALTH*, 18(14).

Han, W., Hou, Y., Yu, Y., Lu, Z., and Qiu, Y. (2022). Fibrous and filmy microplastics exert opposite effects on the mobility of nanoplastics in saturated porous media. *Journal of Hazardous Materials*, page 128912.

Harrison, J. P., Hoellein, T. J., Sapp, M., Tagg, A. S., Ju-Nam, Y., and Ojeda, J. J. (2018). Microplastic-associated biofilms: A comparison of freshwater and marine environments. In *Freshwater Microplastics*, pages 181–201. Springer, Cham.

Hartline, N. L., Bruce, N. J., Karba, S. N., Ruff, E. O., Sonar, S. U., and Holden, P. A. (2016). Microfiber masses recovered from conventional machine washing of new or aged garments. *Environmental science & technology*, 50(21):11532–11538.

He, B., Smith, M., Egodawatta, P., Ayoko, G. A., Rintoul, L., and Goonetilleke, A. (2021). Dispersal and transport of microplastics in river sediments. *ENVIRONMENTAL POLLUTION*, 279.

He, D., Luo, Y., Lu, S., Liu, M., Song, Y., and Lei, L. (2018). Microplastics in soils: Analytical methods, pollution characteristics and ecological risks. *TrAC Trends in Analytical Chemistry*, 109:163–172.

He, L., Rong, H., Wu, D., Li, M., Wang, C., and Tong, M. (2020). Influence of biofilm on the transport and deposition behaviors of nano-and micro-plastic particles in quartz sand. *Water Research*, 178:115808.

Hidalgo, J. J., Neuweiler, I., and Dentz, M. (2021). Transport under advective trapping. *Journal of Fluid Mechanics*, 907:A36.

Hidalgo, J. J., Neuweiler, I., and Dentz, M. (2022). Advective trapping in the flow through composite heterogeneous porous media. *Transport in Porous Media*, 143(3):599–618.

Hou, J., Xu, X., Lan, L., Miao, L., Xu, Y., You, G., and Liu, Z. (2020). Transport behavior of micro polyethylene particles in saturated quartz sand: Impacts of input concentration and physicochemical factors. *Environmental pollution*, 263:114499.

Hu, E., Shang, S., Fu, Z., Zhao, X., Nan, X., Du, Y., and Chen, X. (2020). Cotrans-

port of naphthalene with polystyrene nanoplastics (PSNP) in saturated porous media: Effects of PSNP/naphthalene ratio and ionic strength. *Chemosphere*, 245:125602.

Huang, W., Song, B., Liang, J., Niu, Q., Zeng, G., Shen, M., Deng, J., Luo, Y., Wen, X., and Zhang, Y. (2021). Microplastics and associated contaminants in the aquatic environment: A review on their ecotoxicological effects, trophic transfer, and potential impacts to human health. *Journal of Hazardous Materials*, 405:124187.

Ingraffia, R., Amato, G., Bagarello, V., Carollo, F. G., Giambalvo, D., Iovino, M., Lehmann, A., Rillig, M. C., and Frenda, A. S. (2022). Polyester microplastic fibers affect soil physical properties and erosion as a function of soil type. *Soil*, 8(1):421–435.

Johnson, W. P., Rasmuson, A., Ron, C., Erickson, B., VanNess, K., Bolster, D., and Peters, B. (2020). Anionic nanoparticle and microplastic non-exponential distributions from source scale with grain size in environmental granular media. *Water Research*, 182:116012.

Karadimitriou, NK. and Hassanizadeh, SM. (2012). A review of micromodels and their use in two-phase flow studies. *Vadose Zone Journal*, 11(3):vzj2011–0072.

Kim, JM., Edwards, BJ., Keffer, D. J., and Khomami, B. (2010). Dynamics of individual molecules of linear polyethylene liquids under shear: Atomistic simu-

lation and comparison with a free-draining bead-rod chain. *Journal of Rheology*, 54(2):283–310.

Kim, S.-K., Kim, J.-S., Lee, H., and Lee, H.-J. (2021). Abundance and characteristics of microplastics in soils with different agricultural practices: Importance of sources with internal origin and environmental fate. *Journal of Hazardous Materials*, 403:123997.

Kooi, M. and Koelmans, A. A. (2019). Simplifying microplastic via continuous probability distributions for size, shape, and density. *Environmental Science & Technology Letters*, 6(9):551–557.

Kosuth, M., Mason, S. A., and Wattenberg, E. V. (2018). Anthropogenic contamination of tap water, beer, and sea salt. *PloS one*, 13(4):e0194970.

Kumar, R., Sharma, P., Manna, C., and Jain, M. (2021). Abundance, interaction, ingestion, ecological concerns, and mitigation policies of microplastic pollution in riverine ecosystem: A review. *Science of The Total Environment*, 782:146695.

Lahive, E., Cross, R., Saarloos, A. I., Horton, A. A., Svendsen, C., Hufenus, R., and Mitrano, D. M. (2022). Earthworms ingest microplastic fibres and nanoplastics with effects on egestion rate and long-term retention. *Science of the Total Environment*, 807:151022.

Lanning, L. M. and Ford, R. M. (2002). Glass micromodel study of bacterial dispersion in spatially periodic porous networks. *Biotechnology and bioengineering*, 78(5):556–566.

Lebreton, L., Slat, B., Ferrari, F., Sainte-Rose, B., Aitken, J., Marthouse, R., Hajbane, S., Cunsolo, S., Schwarz, A., Levivier, A., Noble, K., Debeljak, P., Maral, H., Schoeneich-Argent, R., Brambini, R., and Reisser, J. (2018). Evidence that the Great Pacific Garbage Patch is rapidly accumulating plastic. *Scientific Reports*, 8(1):4666.

Li, J., Song, Y., and Cai, Y. (2020). Focus topics on microplastics in soil: Analytical methods, occurrence, transport, and ecological risks. *Environmental Pollution*, 257:113570.

Liu, J., Yang, Y., Ding, J., Zhu, B., and Gao, W. (2019a). Microfibers: A preliminary discussion on their definition and sources. *ENVIRONMENTAL SCIENCE AND POLLUTION RESEARCH*, 26(28, SI):29497–29501.

Liu, J., Zhang, T., Tian, L., Liu, X., Qi, Z., Ma, Y., Ji, R., and Chen, W. (2019b). Aging significantly affects mobility and contaminant-mobilizing ability of nanoplastics in saturated loamy sand. *Environmental Science & Technology*, 53(10):5805–5815.

Liu, T. W. (1989). Flexible polymer chain dynamics and rheological properties in steady flows. *The Journal of chemical physics*, 90(10):5826–5842.

Luo, H., Tu, C., He, D., Zhang, A., Sun, J., Li, J., Xu, J., and Pan, X. (2023). Interactions between microplastics and contaminants: A review focusing on the effect of aging process. *Science of The Total Environment*, page 165615.

Lüscher, S. M. and Jo, H. Y. (2022). A synthetic microplastic fiber-manufacturing method and analysis of airborne microplastic fiber transport behavior in porous media. *Science of The Total Environment*, 838:155888.

Makanga, U., Sepahi, M., Duprat, C., and Delmotte, B. (2023). Obstacle-induced lateral dispersion and nontrivial trapping of flexible fibers settling in a viscous fluid. *Physical Review Fluids*, 8(4):044303.

Margolin, G., Dentz, M., and Berkowitz, B. (2003). Continuous time random walk and multirate mass transfer modeling of sorption. *Chemical Physics*, 295(1):71–80.

Moghani, M. M. and Khomami, B. (2017). Computationally efficient algorithms for Brownian dynamics simulation of long flexible macromolecules modeled as bead-rod chains. *Physical Review Fluids*, 2(2):023303.

Murphy, F., Ewins, C., Carbonnier, F., and Quinn, B. (2016). Wastewater treatment works (WwTW) as a source of microplastics in the aquatic environment. *Environmental science & technology*, 50(11):5800–5808.

Nagel, M., Brun, P.-T., Berthet, H., Lindner, A., Gallaire, F., and Duprat, C. (2018).

Oscillations of confined fibres transported in microchannels. *Journal of Fluid Mechanics*, 835:444–470.

O'Connor, D., Pan, S., Shen, Z., Song, Y., Jin, Y., Wu, W.-M., and Hou, D. (2019). Microplastics undergo accelerated vertical migration in sand soil due to small size and wet-dry cycles. *Environmental Pollution*, 249:527–534.

O'Kelly, B. C., El-Zein, A., Liu, X., Patel, A., Fei, X., Sharma, S., Mohammad, A., Goli, V. S. N. S., Wang, J. J., and Li, D. (2021). Microplastics in soils: An environmental geotechnics perspective. *Environmental Geotechnics*, 8(8):586–618.

Park, J. W., Lee, S. J., Hwang, D. Y., and Seo, S. (2020). Recent purification technologies and human health risk assessment of microplastics. *Materials*, 13(22):5196.

Patrick Wang, P., Zheng, C., and Gorelick, S. M. (2005). A general approach to advective–dispersive transport with multirate mass transfer. *Advances in Water Resources*, 28(1):33–42.

Peller, J. R., Eberhardt, L., Clark, R., Nelson, C., Kostelnik, E., and Iceman, C. (2019). Tracking the distribution of microfiber pollution in a southern Lake Michigan watershed through the analysis of water, sediment and air. *Environmental Science-Processes & Impacts*, 21(9):1549–1559.

Perez, L. J., Parashar, R., Plymale, A., and Scheibe, T. D. (2022). Contributions of

biofilm-induced flow heterogeneities to solute retention and anomalous transport features in porous media. *Water Research*, 209:117896.

Petersen, F. and Hubbart, J. A. (2021). The occurrence and transport of microplastics: The state of the science. *Science of the Total Environment*, 758:143936.

Prata, J. C., da Costa, J. P., Lopes, I., Duarte, A. C., and Rocha-Santos, T. (2020). Environmental exposure to microplastics: An overview on possible human health effects. *Science of the Total Environment*, 702:134455.

Qi, R., Jones, D. L., Li, Z., Liu, Q., and Yan, C. (2020). Behavior of microplastics and plastic film residues in the soil environment: A critical review. *Science of the Total Environment*, 703:134722.

Ranjan, V. P., Joseph, A., Sharma, H. B., and Goel, S. (2023). Preliminary investigation on effects of size, polymer type, and surface behaviour on the vertical mobility of microplastics in a porous media. *Science of The Total Environment*, 864:161148.

Schindelin, J., Arganda-Carreras, I., Frise, E., Kaynig, V., Longair, M., Pietzsch, T., Preibisch, S., Rueden, C., Saalfeld, S., and Schmid, B. (2012). Fiji: An open-source platform for biological-image analysis. *Nature methods*, 9(7):676–682.

Schirinzi, G. F., Pérez-Pomeda, I., Sanchís, J., Rossini, C., Farré, M., and Barceló,

D. (2017). Cytotoxic effects of commonly used nanomaterials and microplastics on cerebral and epithelial human cells. *Environmental Research*, 159:579–587.

Schroeder, C. M. (2018). Single polymer dynamics for molecular rheology. *Journal of Rheology*, 62(1):371–403.

Shi, Y., Huang, H., Zheng, L., Tian, Y., Gong, Z., Wang, J., Li, W., and Gao, S. (2023). Releases of microplastics and chemicals from nonwoven polyester fabric-based polyurethane synthetic leather by photoaging. *Science of The Total Environment*, 902:166584.

Słowicka, A. M., Ekiel-Jeżewska, M. L., Sadlej, K., and Wajnryb, E. (2012). Dynamics of fibers in a wide microchannel. *The Journal of chemical physics*, 136(4):044904.

Sripada, K., Wierzbicka, A., Abass, K., Grimalt, J. O., Erbe, A., Röllin, H. B., Weihe, P., Díaz, G. J., Singh, R. R., and Visnes, T. (2022). A Children's Health Perspective on Nano-and Microplastics. *Environmental health perspectives*, 130(1):015001.

Stanton, T., Johnson, M., Nathanail, P., Gomes, R. L., Needham, T., and Burson, A. (2019). Exploring the efficacy of Nile red in microplastic quantification: A costaining approach. *Environmental Science & Technology Letters*, 6(10):606–611.

Talon, L., Ollivier-Triquet, E., Dentz, M., and Bauer, D. (2023). Transient dispersion regimes in heterogeneous porous media: On the impact of spatial heterogeneity

in permeability and exchange kinetics in mobile–immobile transport. *Advances in Water Resources*, 174:104425.

Waldschläger, K., Lechthaler, S., Stauch, G., and Schüttrumpf, H. (2020). The way of microplastic through the environment – Application of the source-pathway-receptor model (review). *Science of The Total Environment*, 713:136584.

Waldschläger, K. and Schüttrumpf, H. (2020). Infiltration behavior of microplastic particles with different densities, sizes, and shapes—from glass spheres to natural sediments. *Environmental Science & Technology*, 54(15):9366–9373.

Wang, X., Bolan, N., Tsang, D. C. W., Sarkar, B., Bradney, L., and Li, Y. (2021). A review of microplastics aggregation in aquatic environment: Influence factors, analytical methods, and environmental implications. *Journal of Hazardous Materials*, 402:123496.

Xiong, X., Tappenbeck, T. H., Wu, C., and Elser, J. J. (2022). Microplastics in Flathead Lake, a large oligotrophic mountain lake in the USA. *Environmental Pollution*, 306:119445.

Yan, X., Yang, X., Tang, Z., Fu, J., Chen, F., Zhao, Y., Ruan, L., and Yang, Y. (2020). Downward transport of naturally-aged light microplastics in natural loamy sand and the implication to the dissemination of antibiotic resistance genes. *Environmental Pollution*, 262:114270.

Yang, J., Li, L., Li, R., Xu, L., Shen, Y., Li, S., Tu, C., Wu, L., Christie, P., and Luo, Y. (2021a). Microplastics in an agricultural soil following repeated application of three types of sewage sludge: A field study. *ENVIRONMENTAL POLLUTION*, 289.

Yang, L., Zhang, Y., Kang, S., Wang, Z., and Wu, C. (2020). Microplastics in freshwater sediment: A review on methods, occurrence, and sources. *Science of The Total Environment*, page 141948.

Yang, L., Zhang, Y., Kang, S., Wang, Z., and Wu, C. (2021b). Microplastics in freshwater sediment: A review on methods, occurrence, and sources. *Science of the Total Environment*, 754:141948.

Yaseen, A., Assad, I., Sofi, M. S., Hashmi, M. Z., and Bhat, S. U. (2022). A global review of microplastics in wastewater treatment plants: Understanding their occurrence, fate and impact. *Environmental Research*, 212:113258.

Yong, C. Q. Y., Valiyaveettil, S., and Tang, B. L. (2020). Toxicity of microplastics and nanoplastics in mammalian systems. *International Journal of Environmental Research and Public Health*, 17(05):1509.

Zhang, C., Sun, A., Hassan, M. A., and Qin, C. (2022a). Assessing Through-Water Structure-from-Motion Photogrammetry in Gravel-Bed Rivers under Controlled Conditions. *Remote Sensing*, 14(21):5351.

Zhang, Q., Raoof, A., and Hassanizadeh, SM. (2015). Pore-scale study of flow rate on colloid attachment and remobilization in a saturated micromodel. *Journal of Environmental Quality*, 44(5):1376–1383.

Zhang, X., Chen, Y., Li, X., Zhang, Y., Gao, W., Jiang, J., Mo, A., and He, D. (2022b). Size/shape-dependent migration of microplastics in agricultural soil under simulative and natural rainfall. *Science of The Total Environment*, 815:152507.

Zhang, Y.-Q., Lykaki, M., Markiewicz, M., Alrajoula, M. T., Kraas, C., and Stolte, S. (2022c). Environmental contamination by microplastics originating from textiles: Emission, transport, fate and toxicity. *Journal of Hazardous Materials*, page 128453.

Zhou, Y., Wang, J., Zou, M., Jia, Z., Zhou, S., and Li, Y. (2020). Microplastics in soils: A review of methods, occurrence, fate, transport, ecological and environmental risks. *SCIENCE OF THE TOTAL ENVIRONMENT*, 748.